

CERTIFICATION OF APPROVAL

Thermodynamic Model for Relating Volumetric to Mass Flow Rate for Natural Gas

by

Siti Aishah Binti Sahari

A project dissertation submitted to the
Chemical Engineering Programme
University Teknologi PETRONAS
In partial fulfillment of the requirement for the
BACHELOR OF ENGINEERING (Hons)
(CHEMICAL ENGINEERING)

Approved by,



(AP Dr. Mohamed Ibrahim b. Abdul Mutalib)

UNIVERSITI TEKNOLOGI PETRONAS
TRONOH, PERAK

January 2005

PUSAT SUMBER MAKLUMAT
UNIVERSITI TEKNOLOGI PETRONAS

UNIVERSITI TEKNOLOGI PETRONAS
Information Resource Center



IPB181039

CERTIFICATION OF ORIGINALITY

This is to certify that I am responsible for the work submitted in this project, that the original work is my own except as specified in the references and acknowledgements, and that the original work contained herein have not been undertaken or done by unspecified sources or persons.



SITI AISHAH BINTI SAHARI

ABSTRACT

This project presents a method of measuring mass flow rate of natural gas using a reliable Equation of State (EOS) to eliminate the use of expensive coriolis meter. Natural gas is an alternative vehicle fuel that has long been proposed as a way to provide significant air quality benefits over petroleum fuels. Unlike gasoline or diesel gas that can be measured in volumetric flow rate, natural gas needs to be measured in mass flow rate. Only coriolis meter is available in the market that can give the reading in mass per unit time while the other flow meters give the volumetric reading. However, the high cost of coriolis meter has led to the research of finding another alternative to measure mass flow rate of natural gas. The method considered in the study is to have the volumetric flow rate measured, prior to converting it to mass flow rate using a suitable Equation of State (EOS).

In order to complete this project, there are four critical stages involved. The first stage is to conduct several experiments using a Test Rig Dispenser to obtain Pressure-Volume-Temperature (PVT) relation of natural gas. These data are then being used for the purpose of performing computation of errors for the tested EOSs. Errors for all of the EOSs are then compared to determine the EOS that gives the smallest error percentage. After that, another stage to validate the obtained EOS is done. In this stage, the EOS is used along with PVT data to compute mass flow rate of the natural gas dispensed. This mass flow rate from the computation is then being compared to the measured value of coriolis meter.

From the results of dynamic experiment, it is observed that ideal gas law gives smallest error percentage followed by SRK, Lee-Kesler, Peng-Robinson, Van der Waals and Virial equation of state. However, from the static experiment, SRK gives the smallest error followed by Lee-Kesler Plocker, Peng-Robinson, Van der Waals, Virial, and ideal gas equation. The static experiment gives more accurate result since all thermodynamic properties are taken at their steady state condition.

ACKNOWLEDGEMENTS

I would like to express my heartfelt thanks and gratitude to those who had contributed to the success of my final year research project at University Technology Petronas. Proceeding with particular order, my thanks go to my supervisor, AP Dr. Mohamed Ibrahim b. Abdul Mutalib for his guidance and commitment in overseeing the success of this project from the beginning to the end.

I am also especially in depth to the Head of Department of Chemical Engineering, Dr Helmy and the coordinator of Final Year Research Project, Puan Yuliana, for their time and effort in overseeing the progress of the entire project and also in providing me with the necessary resources.

Next special thanks goes to librarians of University Technology Petronas for being very helpful for me to search for journals and reference books in completing the project. I would also like to thank research officer of Natural Gas Refueling System Project namely Mahidzal Dahari for his assistance in conducting the experiments.

Last but not least, my gratitude goes to my parents, my siblings and my friends for their mental support and advice in dealing with many difficulties faced during this period of time. Their help in providing assistance for acquiring important information and resources is also appreciated.

TABLE OF CONTENTS

CERTIFICATION.....	i
ABSTRACT.....	iii
TABLE OF CONTENTS.....	1
CHAPTER 1	5
INTRODUCTION	5
1.1 Background of Study	5
1.2 Problem Statement.....	6
1.3 Objectives and Scopes of Study.....	7
CHAPTER 2	8
LITERATURE REVIEW	8
2.1 Natural Gas Vehicle.....	8
2.1.1 Physical Properties and Production	9
2.1.2 Energy Storage Density and Storage Cost.	9
2.1.3 CNG Vehicle Fuel Systems	10
2.1.4 Fuel Costs.....	11
2.1.5 Emissions	12
2.1.6 Greenhouse Gases.....	13
2.2 Previous Works on Application of Equation of State for Natural Gas	14
2.2.1 Calculations of volumetric properties.....	14
2.3 Equation of State (EOS).....	16
2.3.1 Ideal Gas Equation.....	16
2.3.2 The Virial Equation.....	17
2.3.3 Van der Waal Equation.....	18
2.3.4 Redlich-Kwong Equation of State	19
2.3.5 The Soave-Redlich Kwong (SRK) Equation	19
2.3.6 Peng-Robinson Equation of State	19
2.3.7 Lee Kesler Plocker Equation	20
2.4 Joule-Thompson Effect.....	20

CHAPTER 3	22
METHODOLOGY	22
3.1 Experiment using NGV Dispenser Test Rig.....	22
3.1.1 Equipment Overview	22
3.1.2 Process Flow Description	24
3.2 Computation of Error for EOS.....	27
3.2.1 Natural Gas Properties	29
3.2.4 Ideal Gas Error Computation	34
3.2.5 Van der Waals Error Computation	34
3.2.6 Peng-Robinson Error Computation.....	35
3.2.7 Soave-Redlich-Kwong (SRK) Error Computation	35
3.2.8 Virial Error Computation.....	35
3.2.9 Lee-Kesler Error Computation	36
3.3 Validation.....	37
CHAPTER 4	42
RESULTS AND DISCUSSION	42
4.1 Dynamic Experiment	42
4.1.1 Experiment 1-4 (One Continuous Flow of Natural Gas into the Vehicle Tank).....	42
4.1.2 Experiment 5 (Several Continuous Flow of Natural Gas into the Vehicle Tank).....	47
4.2 Static Experiment.....	49
4.3 Validation.....	52
CHAPTER 5	54
CONCLUSIONS AND RECOMMENDATIONS	54
REFERENCES	56

TABLE OF FIGURES

Figure 1: Volume Needed to Store Equal Amounts of Energy, CNG Compared to Gasoline	9
Figure 2: Light-Duty CNG Vehicle Exhaust Emissions.....	12
Figure 3: Various parts of the NGV Dispenser Test Rig.....	24
Figure 4: Simplified flow diagram of NGV Dispenser Test Rig.....	25
Figure 5: Steps for error computation of EOSs	28
Figure 6: Data required by software	37
Figure 7: Results from computation	37
Figure 8: Systematic steps in validation technique.....	38
Figure 9: Command to find roots of equation using MATLAB program.....	40
Figure 10: Roots of equation for the first experiment.....	41
Figure 11: Graph of error versus time for experiment 1	43
Figure 12: Graph of error versus time for experiment 2	44
Figure 13: Graph of error versus time for experiment 3	44
Figure 14: Graph of error versus time for experiment 4	45
Figure 15: Graph of pressure inside the vehicle tank versus time for Experiment 1	46
Figure 16: Graph of mass of natural gas versus time for Experiment 1	46
Figure 17: Graph of temperature inside the vehicle tank versus time for Experiment 1 ..	46
Figure 18: Graph of error versus time for experiment 5	47
Figure 19: Graph of pressure inside the vehicle tank versus time for Experiment 5	48
Figure 20: Graph of mass of natural gas versus time for Experiment 5	48
Figure 21: Graph of temperature inside the vehicle tank versus time for Experiment 5 ..	48
Figure 22: Graph of error versus time for experiment 6.....	50
Figure 23: Graph of error versus time for experiment 7.....	50
Figure 24: Graph of error versus time for experiment 8.....	51
Figure 25: Pressure of NG inside the tank for Static Experiment (Exp. 6)	51
Figure 26: Mass of NG inside the tank for Static Experiment (Exp. 6).....	52
Figure 27: Temperature of NG inside the tank for Static Experiment (Exp. 6).....	52

Figure 28: Comparison of coriolis and experimental value of mass flow rate for natural gas for Experiment 1 53

LIST OF TABLES

Table 1: Annual Miles Traveled to Achieve Three-Year Simple Payback of a CNG Fuel System1 at Various Fuel Economics and Equivalent Gallon CNG Price Differentials ... 11

Table 2: Compositions of Natural Gas (Leanest and Richest)..... 30

Table 3: Average Composition of Natural Gas..... 30

Table 4: Molecular Weight of Natural Gas components 31

Table 5: Critical Pressure and Temperature of Natural Gas Components..... 32

Table 6: Acentric factor of Natural Gas Components 33

Table 7: Properties of Natural Gas..... 34

CHAPTER 1

INTRODUCTION

1.1 BACKGROUND OF STUDY

Automotive industry is one of the fastest growing industries in the world. This results to the production of million of highway vehicles that operate every single day which in turn imposes severe environmental problems to the world. Emissions from millions of cars and light-duty trucks, almost exclusively operating on gasoline and diesel fuel, are major contributors to this problem. In addition, heavy-duty trucks and buses using diesel fuel are major sources of particulates (small unburned particles of hydrocarbons and sulfur) and nitrogen oxide emissions in urban areas. Particulates are a special concern because the public is frequently exposed to them and current research suggests significant respiratory problems and cancer-causing potential from particulates (Bechtold, 1997).

Alternative vehicle fuels such as natural gas, methanol, ethanol, propane, and electricity have long been proposed as a way to provide significant air quality benefits over petroleum fuels. However, great interest is given to natural gas vehicle technology. Significant advances have been made in the past few years that have highlighted the efficiency and emissions potential of natural gas vehicles. In transportation sector, natural gas is becoming more important. It may be used in two forms: compressed natural gas (CNG) and liquefied natural gas (LNG). Fundamentally, the difference between these two forms is energy density - a liquid fuel carries more energy per pound than a gaseous fuel.

Compressed Natural Gas Vehicle (CNGV) has many overwhelming advantages against traditional means of transportation using gasoline and diesel. Firstly, it brings environmental benefits because natural gas is completely burnt in comparison to gasoline, alcohol or diesel. This is why NGVs emit less pollutant, i.e. nitrous oxides (NO_x), carbon

dioxide (CO₂) and especially carbon monoxide (CO). Secondly, the natural gas resource is more abundant, which makes the fuel cost lower than gasoline. Besides, it is a safer fuel. As natural gas is lighter than air, in the case of leakage, it dissipates into the atmosphere, thereby reducing the risk of explosions and fires.

1.2 PROBLEM STATEMENT

Sales and purchases of gas involve a flow of money into and out of the industry; hence accurate flow measurement is of paramount importance. A slight error will caused a loss of million either to the seller or purchaser. Unlike gasoline or diesel which can be measured in volumetric flow rate, natural gas needs to be measured in mass flow rate. This is because unlike liquid, volume of gas is affected by its temperature and pressure. The higher temperature and the lower pressure, the greater the volume of gas will be. Several types of flow meter are available in market such as coriolis meter, vortex flow meter, positive displacement flow meter and differential meter. Among this four, only coriolis meter give the reading in mass per unit time while the other flow meters give the volumetric reading. However, the high cost of coriolis meter has led to the research of finding alternative measurement to mass flow rate of natural gas. The method considered in the study is to have the volumetric flow rate measured, prior to converting it to mass flow rate using a selected Equation of State (EOS).

1.3 OBJECTIVES AND SCOPES OF STUDY

The project is relevant through the light of its objectives and scope of study. The main objectives of the study are:

- i. To find the relation of pressure, temperature and mass for the natural gas system through series of experiments conducted using a NGV Dispenser Test Rig.
- ii. To find the best Equation of State (EOS) that can represents the natural gas system from several EOSs such as ideal gas, Virial, Van der Waal, Peng-Robinson, Soave-Redlich-Kwong and Lee-Kesler equations.
- iii. To validate the EOS that had been selected from the calculation using coriolis meter measurements as a reference.

The scope of this study will focus on finding the best EOS that can describes the relationship between the volume of natural gas and its pressure and temperature using experimental data, in order to relate volumetric to mass flow rate for natural gas.

1.3.1 The Relevancy of the Project

The project is an opportunity for the author to gain knowledge on some thermodynamics properties such as pressure, temperature and volume of natural gas and the development of natural gas vehicle. From the university's perspective, the project is part of a project conducted by University Technology Petronas (UTP) on the development of natural gas refueling system.

1.3.2 Feasibility of the Project Within the Scope and Time Frame

The scope of the project is viable for completion in a one-semester research project. Approximately one-third of the duration was spent on conducting experiments, another one-third on computations of errors for several EOSs, and the final one-third for validation of the best EOS obtained from the error computation results.

CHAPTER 2

LITERATURE REVIEW

2.1 NATURAL GAS VEHICLE

Natural Gas Vehicle (NGV) is one of the alternative fuels for vehicles that have been considered as a way to provide significant air quality benefits over petroleum fuels such as gasoline and diesel. Natural gas has unique physicochemical properties, and there are vast reserves of the material, with a highly developed network for supplying it from deposits to many regions over major gas pipelines, which combine with a low price and considerable ecological advantages by comparison with traditional fuels, all of which make NG a universal vehicle fuel for the 21st century (Kirillov, 2001).

2.1.1 Physical Properties and Production

Natural gas is composed primarily of methane, with a small percentage of ethane and minute amounts of propane and heavier hydrocarbons typically present. Natural gas also can include small amounts of nitrogen, carbon dioxide (CO₂), and oxygen. Impurities can include water vapor, hydrogen sulfide, and entrained particulates (Bechtold, 1997).

2.1.2 Energy Storage Density and Storage Cost.

The amount of energy in a unit volume of natural gas is much less than in the same volume of gasoline. For vehicle use, the same natural gas that is distributed at very low pressures for heating and cooking is compressed and stored as CNG in specially designed tanks at pressures of 2,400 to 3,600 psi (Bechtold, 1997). *Figure 1* illustrates the difference in energy storage density for CNG versus gasoline. Besides needing three to five times the volume for storage, CNG storage cylinders are much heavier than gasoline tanks and are more difficult to place within the vehicle because of their cylindrical shape.

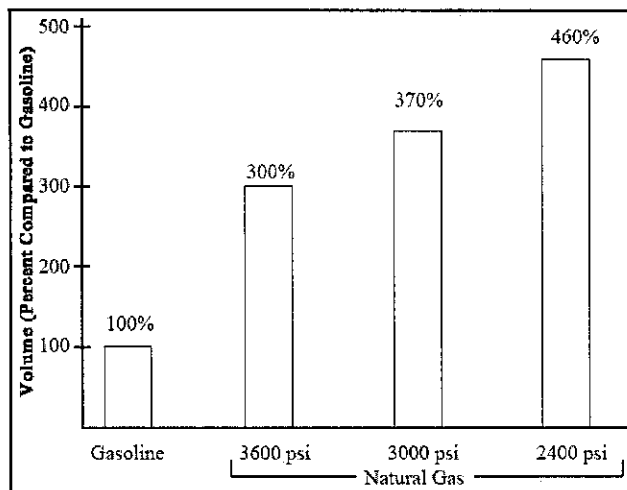


Figure 1: Volume Needed to Store Equal Amounts of Energy, CNG Compared to Gasoline

Source: Alternative Fuels for Vehicles Fleet Demonstration Program

To reduce the weight of CNG tanks, manufacturers in recent years have introduced lighter materials. To store the CNG equivalent of 10 gallons of gasoline, steel-reinforced CNG cylinders would weigh about 260 pounds, aluminum-reinforced CNG cylinders would weigh about 220 pounds, and all-composite (made from combinations of carbon fiber and other advanced materials) cylinders would weigh about 110 pounds. By comparison, the empty weight of a 10-gallon gasoline tank is only 20 to 30 pounds (depending on the shape of the tank and the material used), and its cost is relatively very low (Bechtold, 1997).

2.1.3 CNG Vehicle Fuel Systems

Just as tanks have evolved, natural gas fuel systems have evolved tremendously over the past few years as the popularity of natural gas vehicles grown. The oldest-style natural gas fuel systems reduce the pressure of the gas coming from the CNG tanks and employ simple mechanical mechanisms to mix the natural gas with the air entering the engine. Bechtold (1997) indicates that this type of fuel system operates without electronic controls and is known as an “open-loop” system because it does not monitor the oxygen content of the exhaust gases to adjust the ratio of fuel to air entering the engine. Second-generation CNG fuel systems incorporates oxygen sensor in the engine exhaust to adjust the ratio of fuel to air entering the engine and are known as "closed-loop" systems. The

most advanced CNG fuel system technology, as found in dedicated CNG vehicles built by vehicle manufacturers, is essentially the same as the prevalent multipoint fuel injection systems found in almost all new gasoline vehicles. The primary difference is that the injectors are optimized to use natural gas instead of gasoline. Most CNG fuel systems currently in service were designed to be installed on a gasoline vehicle while retaining the gasoline fuel system. This bifuel approach allows the driver to change from one fuel to the other by flipping a switch (the vehicle can only use one fuel at a time), or the vehicle can be set up to switch automatically to gasoline when the CNG is depleted. Bifuel configurations were adopted for two reasons:

- the difficulty of incorporating enough CNG fuel storage to equal the operating range on gasoline; and
- the scarcity of places to refuel with CNG, other than the home base of the vehicle.

Auto manufacturers recognize that bifuel CNG vehicles can play an important role in creating demand for CNG refueling infrastructure, and have decided to assist by offering vehicles especially configured to become bifuel vehicles. The only difference in these vehicles is that a few engine modifications have been made in the interests of engine durability when using natural gas, and a smaller gasoline fuel tank is usually installed, creating more room for CNG cylinders.

2.1.4 Fuel Costs.

In most cases, the cost of an equivalent amount of CNG is less than gasoline, resulting in lower fuel operating costs. *Table 1* lists the miles a vehicle would have to travel to achieve a three-year simple payback of a typical CNG fuel system costing \$4,500 (or a CNG vehicle with an incremental cost of \$4,500) for various vehicle fuel economies and fuel-price differentials. For example, a vehicle with a fuel economy of 15 miles per gallon (mpg) would have to travel 90,000 miles per year to achieve three-year simple payback, if CNG were priced 25 cents per gallon lower than gasoline. As *Table 3.3* indicates, only a vehicle that uses large quantities of fuel, either because the vehicle has

with the gasoline fuel and emissions-control systems; if poorly integrated, emissions increases can occur.

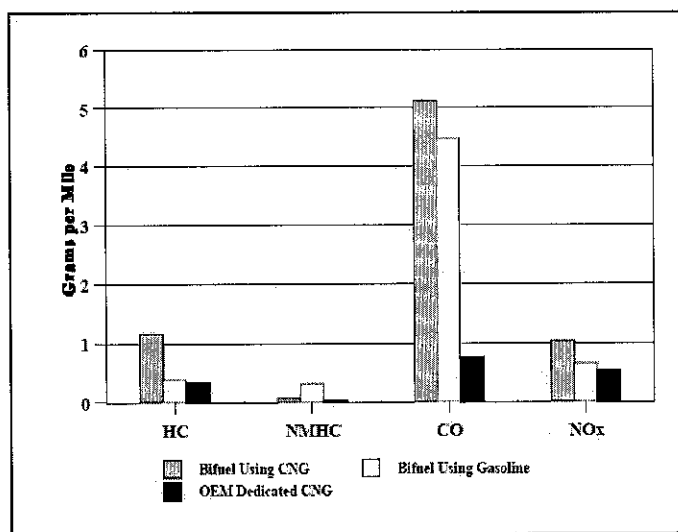


Figure 2: Light-Duty CNG Vehicle Exhaust Emissions

Source: Alternative Fuels for Vehicles Fleet Demonstration Program

Figure 2 illustrates the average tailpipe emissions of both bifuel (CNG and gasoline) and some original equipment manufacturer (OEM) dedicated CNG vehicles. The bifuel data include tests of a wide assortment of CNG conversion systems, some of which performed poorly in emissions tests. The OEM dedicated CNG vehicles demonstrated the lowest emissions across the board. This performance by dedicated CNG vehicles is even more impressive considering that these vehicles, unlike gasoline vehicles and the gasoline systems on bifuel CNG vehicles, do not produce evaporative, running loss, or refueling emissions. For the bifuel vehicles, CNG did not provide across-the-board tailpipe emissions reductions compared to gasoline. Total hydrocarbons (HC) were higher when using CNG since methane is more difficult to oxidize in catalytic converters than typical gasoline hydrocarbons. Non-methane hydrocarbon (NMHC) emissions when using CNG were much lower than when using gasoline, but CO and NO_x emissions were higher. After adjusting for how emissions react in the atmosphere to form ozone, the ozone-forming potential of CNG vehicle exhaust is estimated to be only about half that of gasoline vehicle exhaust. In addition, evaporative, running loss, and refueling emissions of late-model gasoline vehicles are estimated to be nearly 50% higher than their exhaust

hydrocarbon emissions. Dedicated CNG vehicles thus should have overall ozone-forming potential that is 80 to 85% lower than gasoline vehicles. Bifuel vehicles should have from one-half to three-quarters of the ozone-forming potential of gasoline vehicles because the gasoline carried by bifuel vehicles causes evaporative, running loss, and refueling emissions (Bechtold, 1997).

2.1.6 Greenhouse Gases

Vehicles using natural gas have an inherent advantage in CO₂ emissions compared to vehicles using gasoline. This is because natural gas contains more hydrogen and less carbon than gasoline. According to Wang (1996), for vehicles of equal fuel efficiency, natural gas produces only about 75% of the CO₂ emissions. (This advantage is reduced in bifuel vehicles where CNG fuel efficiency is lower than that of gasoline.) When the entire fuel cycle from resource through combustion (full fuel cycle) is taken into account, along with the other greenhouse gases, a dedicated CNG vehicle has an overall estimated greenhouse gas impact that is up to 15% less than that of a similar gasoline vehicle.

2.2 PREVIOUS WORKS ON APPLICATION OF EQUATION OF STATE FOR NATURAL GAS

2.2.1 Calculations of volumetric properties

In this section the most widely used methods to calculate compressibility factor and density of natural gas are presented.

Correlations

The standard method of calculating compressibility factor for natural gases is based on finding pseudo-critical properties of the gases via mixing rules such as Stewart–Burkhardt–Voo (1959) (SBV) mixing rule.

$$J = \left(\frac{1}{3}\right) \left[\sum y_i \left(\frac{T_c}{P_c} \right)_i \right] + \left(\frac{2}{3}\right) \left[\sum y_i \left(\frac{T_c}{P_c} \right)_i^{0.5} \right]^2 \quad (2-1)$$

$$K = \sum \left[y_i \left(\frac{T_c}{P_c^{0.5}} \right)_i \right] \quad (2-2)$$

Sutton (1985) found that SBV method results in a large deviation in estimating the Z-factor for gases with high content of C₇₊. The following corrections are proposed to minimize this deviation.

$$F_j = \left(\frac{1}{3}\right) \left[y \left(\frac{T_c}{P_c} \right) \right]_{C_{7+}} + \left(\frac{2}{3}\right) \left[y \left(\frac{T_c}{P_c} \right)^{0.5} \right]_{C_{7+}}^2 \quad (2-3)$$

$$E_j = 0.6081 F_j + 1.1325 F_j^2 - 14.004 F_j y_{C_{7+}} + 64.434 F_j y_{C_{7+}}^2 \quad (2-4)$$

$$E_k = \left(\frac{T_c}{P_c^{0.5}} \right)_{C_{7+}} \left[0.3129 y_{C_{7+}} - 4.8156 y_{C_{7+}}^2 + 27.3751 y_{C_{7+}}^3 \right] \quad (2-5)$$

$$J' = J - E_j \quad (2-6)$$

$$K' = K - E_k \quad (2-7)$$

The corrected pseudo-critical temperature and pressure are calculated from *Equations (2-8) and (2-9)* as follows:

$$T_{pc} = \frac{K'^2}{J'} \quad (2-8)$$

$$P_{pc} = \frac{T_{pc}}{J'} \quad (2-9)$$

If the natural gases are sweet, containing neither hydrogen sulfide nor carbon dioxide, then the pseudo-critical temperature and pressure are used to calculate pseudo-reduced properties from *Equations (8) and (9)*. However, natural gases frequently contain hydrogen sulfide, carbon dioxide, and/or nitrogen that affect the accuracy of the value of Z-factor calculated using Standing–Katz (1942) charts. Wichert and Aziz (1972) presented a method to correct the pseudo-critical properties of natural gases to the presence of these non-hydrocarbon components. The correction factor is:

$$\epsilon = 120(A^{0.9} - A^{1.6}) + 1.5(B^{0.5} - B^4) \quad (2-10)$$

where the coefficient *A* is the sum of the mole fraction of H₂S and CO₂ and *B* the mole

fraction of H₂S in the gas mixture. The corrected pseudo-critical properties P'_{pc} and T'_{pc} are:

$$T'_{pc} = T_{pc} - \epsilon \quad (2-11)$$

$$P'_{pc} = \frac{P_{pc} T'_{pc}}{[T_{pc} + B(1-B)\epsilon]} \quad (2-12)$$

The pseudo-reduced pressure and temperature are expressed by the following relationship:

$$P_{pr} = \frac{P}{P_{pc}} \quad (2-13)$$

$$T_{pr} = \frac{T}{T_{pc}} \quad (2-14)$$

EOS calculations of volumetric properties

Several forms of EOS have been presented to calculate hydrocarbon fluid properties. These EOS can be written in general form as:

$$P = \frac{RT}{v-b} - \frac{a}{v^2 + uv - w^2} \quad (2-15)$$

In the above equation p is the pressure, R the gas constant, T the absolute temperature, v the molar volume, and u and w are constants. The parameters a and b are constants characterizing the molecular properties of the individual component. The parameter a is a measure of the intermolecular attraction and b represent the molecular size. In two-parameter EOS, u and w are related to b whereas in a three-parameter EOS u and w are related to a third parameter c . The two parameters EOS is the most popular one, where a and b are expressed as a function of critical properties as:

$$a = \frac{\Omega_a R^2 T_c^2}{P_c} \quad (2-16)$$

$$b = \frac{\Omega_b R T_c}{P_c} \quad (2-17)$$

where Ω_a and Ω_b are constants having different values for different EOS. Elsharkawy (2003) suggested that the most widely used EOS are Soave–Redlich–Kwong (SRK-EOS) and Peng–Robinson (PR-EOS). The two parameters EOS predict the same critical

compressibility factor, Z_c for all pure components, whereas Z_c varies within a range of 0.2–0.3 for all hydrocarbon components.

2.3 EQUATION OF STATE (EOS)

A gas may be defined as a homogeneous fluid of low density and low viscosity, which has neither independent shape nor volume but expands to fill completely the vessel in which it is contained. The properties of the molecules in gases differ considerably from the properties of liquids, mainly because the molecules in gases are much further apart than molecules in liquids. For instance, a change in pressure has a much greater effect on the density of a gas than of a liquid. There are several equations used to describe the relationship between the volume of a gas and its pressure and temperature. The term *equation of state* is used to indicate an equation which relates volume to pressure and temperature.

2.3.1 Ideal Gas Equation

The simplest equation that relates mass and volume for gas is the ideal gas equation:

$$PV = nRT \quad (2-18)$$

All substances behave according to this simple equation at sufficiently high specific volume (low density). This is because, at vanishingly low density, the individual molecules are essentially “point particles”, occupying zero volume and never colliding with one another (Winnick, 1997).

In engineering applications, which are most often at atmospheric pressure or higher, no fluid is truly an ideal gas. However in many cases the assumption is within a few percent to be exact.

2.3.2 The Virial Equation

The virial equation of state has a sound theoretical foundation; it can be derived from first principles using statistical mechanics. This equation is given by a power series expansion for the compressibility factor in density (or the reciprocal of volume) about $1/v=0$;

$$z = \frac{Pv}{RT} = 1 + \frac{B}{v} + \frac{C}{v^2} + \frac{D}{v^3} + \dots \quad (2-19)$$

Here, B, C, ... are called the second, third, virial coefficients; these parameters depend only on temperature (and the composition for mixtures). An alternative expression for the virial equation is a power series expansion in pressure:

$$z = \frac{Pv}{RT} = 1 + B'P + C'P^2 + D'P^3 + \dots \quad (2-20)$$

By solving the first equation for P and substituting into the second equation, it is straightforward to show the two sets of coefficients are related by:

$$B' = \frac{B}{RT} \quad (2-21)$$

$$C' = \frac{C - B^2}{(RT)^2} \quad (2-22)$$

It turns out that at moderate pressures (up to about 15 bar), the power series expansion in pressure is better when only the second virial coefficient is used.

$$z = \frac{Pv}{RT} = 1 + B'P = 1 + \frac{BP}{RT} \quad (2-23)$$

From 15 to 50 bar, the virial coefficient should contain three terms, and the expansion in density is more accurate:

$$z = 1 + \frac{B}{v} + \frac{C}{v^2} \quad (2-24)$$

Using statistical mechanics, we can relate the virial coefficients to intermolecular potentials. The second virial coefficient, B, results from all the “two-body” interactions in the system, that is, all the interactions between two molecules; the third virial coefficient, C, results from all the “three-body” interactions in the system; and so on. From this point of view, we can see that we need to include more and more terms as the pressure increases (Sandler, 1999).

2.3.3 Van der Waal Equation

The van der Waals equation of state is arrived at from the ideal gas by first adding a term representative of intermolecular attraction, a/v^2 , where a is an empirical constant specific for each substance. This force has some theoretical justification; the attractive “London” forces between molecules, which exist because of mutually induced perturbations in their electron clouds, decay with the sixth order in intermolecular distance. The square of the molar volume is roughly proportional to this distance raised to the sixth power. It is this force, which increases sharply in magnitude as the volume decreases, that is responsible for condensation.

The second modification is the addition of a term, b , specific to each substance, and representative of the hard volume of the molecules themselves, that is, a volume below which the system can never be compressed (Winnick, 1997). The resulting equation is:

$$P = \frac{RT}{v-b} - \frac{a}{v^2} \quad (2-25)$$

2.3.4 Redlich-Kwong Equation of State

An empirical modification to the van der Waals equation was made by Otto Redlich. He found that, whereas the first term in van der Waals equation was a reasonable assessment of the repulsive forces, the attractive-force term needed temperature dependence to reproduce a large quantity of experimental data more accurately. He tested a number of modifications, eventually settling on (Winnick, 1997):

$$P = \frac{RT}{v-b} - \frac{a}{\sqrt{T}v(v+b)} \quad (2-26)$$

2.3.5 The Soave-Redlich Kwong (SRK) Equation

The Redlich-Kwong equation is reasonably good at describing liquid and vapor volumes, but when the process is inverted and vapor pressures are predicted, the results are severely in error. This led Soave to replace the constant a with one that was dependent on temperature; he further put in a dependence on the acentric factor, ω , which in its development, was based on vapor pressure behavior. The result is an equation that is not

much better in predicting volumes, but is far better in predicting vapor pressures of pure components.

The form of the SRK equation:

$$P = \frac{RT}{v-b} - \frac{a\alpha}{v(v+b)} \quad (2-27)$$

is basically the same as the Redlich-Kwong equation, but with the a now being temperature dependent (Winnick, 1997).

2.3.6 Peng-Robinson Equation of State

$$P = \frac{RT}{v-b} - \frac{a\alpha}{v^2 + 2bv - b^2} \quad (2-28)$$

Peng Robinson equation is related to the SRK and was developed to overcome the instability in the SRK equation near the critical point. This correlation provides reasonable accuracy near critical point. It is commonly used to represent hydrocarbon and inorganic gases such as nitrogen, oxygen and hydrogen sulfide (Sandler, 1999).

2.3.7 Lee Kesler Plocker Equation

Benedict Webb Rubin is an equation of state that has eight empirical constants and gives accurate predictions for vapor and liquid phase hydrocarbons. It can also be used for mixtures of light hydrocarbons with carbon dioxide and water.

$$P = \rho RT + \left(B_0 RT - A_0 - \frac{C_0}{T^2} + \frac{D_0}{T^3} - \frac{E_0}{T^4} \right) \rho^2 + \left(bRT - \alpha - \frac{d}{T} \right) \rho^3 + \alpha \left(\alpha + \frac{d}{T} \right) \rho^6 + \frac{c\rho^3}{T^2} (1 + \gamma\rho^2) \exp(-\gamma\rho^2) \quad (2-29)$$

Lee and Kesler extended the Benedict Webb Rubin equation to a wider variety for substance using the principle of corresponding state. The method was modified further by Plocker. A new method to calculate critical properties and other constant were introduced (Sandler, 1999).

$$Tc_{ij} = (Tc_i Tc_j)^{1/2} \quad (2-30)$$

$$Tc_{ii} = Tc_i \quad (2-31)$$

$$Vc_m = \sum_i \sum_j x_i x_j Vc_{ij} \quad (2-32)$$

$$Vc_{ij} = \frac{1}{8} (Vc_i^{1/3} + Vc_j^{1/3})^3 \quad (2-33)$$

$$Vc_i = Zc_i \frac{RTc_i}{Pc_i} \quad (2-34)$$

$$Zc_i = 0.2905 - 0.085 \omega_i \quad (2-35)$$

$$Zc_m = 0.2905 - 0.085 \omega_m \quad (2-36)$$

$$Pc_m = Zc_m \frac{RTc_m}{Vc_m} \quad (2-37)$$

$$\omega_m = \sum_i x_i \omega_i \quad (2-38)$$

2.4 JOULE-THOMPSON EFFECT

Temperature changes as pressure is reduced when a flowing stream of gas passes through a throttle, valve, choke, or perforations in casing. This is called the Joule-Thompson Effect. The change in temperature is directly related to the attraction of the molecules for each other. The equation

$$\Delta T = \frac{T \left(\frac{\partial V_M}{\partial T} \right)_p - V_M}{C_p} \Delta p \quad (2-39)$$

gives the change in temperature as pressure is changed. This equation is valid when the pressure change is adiabatic, that is, no heat enters or leaves the system, and when pressure change is small.

Substitution of the compressibility equation of state

$$pV_M = zRT \quad (2-40)$$

into Equation 2-39 results in

$$\Delta T = \frac{\frac{V_M T}{z} \left(\frac{\partial z}{\partial T} \right)_p - V_M}{C_p} \Delta p \quad (2-41)$$

The terms V, T, z and C_p are always positive. Thus, the direction of the change in temperature depends on the signs of both the Δp term and the derivative, $(\delta z/\delta T)_p$.

At moderate pressure, say values of pseudoreduced pressure less than about 6.0, z -factor increases as temperature increases at constant pressure. That is, at pseudoreduced pressures less than about 6.0, the derivative of z -factor with respect to T is positive. Use of a negative value of Δp and a positive value of $(\delta z/\delta T)_p$ in Equation 2-41 causes ΔT to be negative. That is temperature decreases as pressure decreases.

CHAPTER 3

METHODOLOGY

In order to complete this project, there are four critical stages involved. The first stage is to conduct several experiments using a Test Rig Dispenser. This equipment is built specifically for the purpose of developing and conducting research for the natural gas dispensing system. Having done the experiments, data obtained such as pressure, temperature and mass of natural gas are collected. These data are then being used for the purpose of performing computation of errors for the tested EOSs. Errors for all of the EOSs are then compared to determine the EOS that gives the smallest error percentage. This EOS is considered as the best EOS that can be applied for the natural gas system. After that, another stage to validate the obtained EOS is done. In this stage, the EOS is used along with some experimental data such as volumetric flow rate, pressure and temperature to compute mass flow rate of the natural gas dispensed. This mass flow rate from the computation is then being compared to the measured value of coriolis meter. Next, error between these two values is calculated to determine the reliability of the EOS.

3.1 EXPERIMENT USING NGV DISPENSER TEST RIG

3.1.1 Equipment Overview

The NGV Dispenser test rig is designed in such that it shall be able to replicate the actual filling condition of a commercial filling station. The NGV Dispenser Test Rig consists of storage cylinders horizontally stacked in metal frame, panel mounted dispenser, slow-filled compressor, gas piping, electrical control and data acquisition system.

The high pressure natural gas is stored inside storage cylinders at 3600 psig. After the dispenser start button is switched on, the gas flows from the storage cylinders to the dispenser and finally to a tank which is considered as a vehicle tank. The sequencing is done automatically via dispenser control and the total amount of gas flow to the vehicle

tank is registered on a display panel. There are four types of flow meters installed in the dispensing system which are coriolis, vortex, differential pressure and turbine with coriolis flow meter used as the master reference. While dispensing gas to the vehicle tank, all process parameters such as pressures, temperatures and flow rates are being transmitted to a data acquisition system (DAQ). DAQ will then process the data and produce tables and charts.

Recycling system is used to empty the vehicle tank by transferring the gas to the storage cylinders. This is done via slow-filled compressor that has the inlet and discharge pressure of 1.25 psig and 3600 psig respectively. Once empty, the compressor will stop and the next sampling process could take place. *Figure 3* below shows some pictures of the various parts of the NGV Dispenser Test Rig.

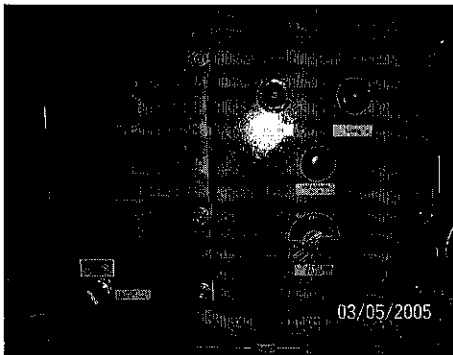


Figure 3-1a: Start switch panel

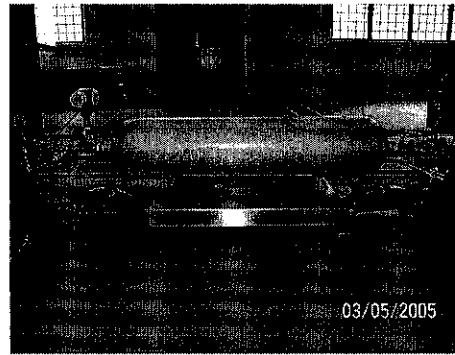


Figure 3-1b: Vehicle tank

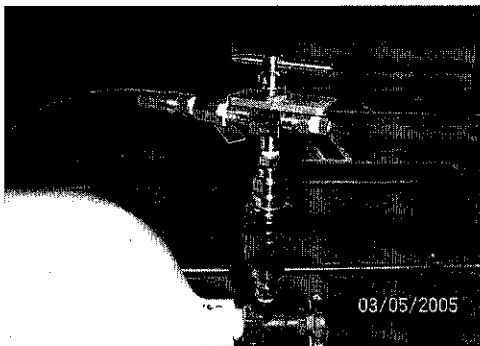


Figure 3-1c: Nozzle connected to vehicle tank.

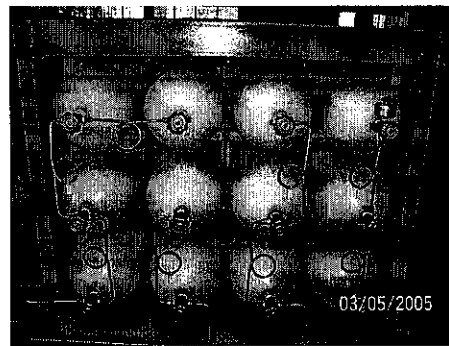


Figure 3-1d: Storage tanks

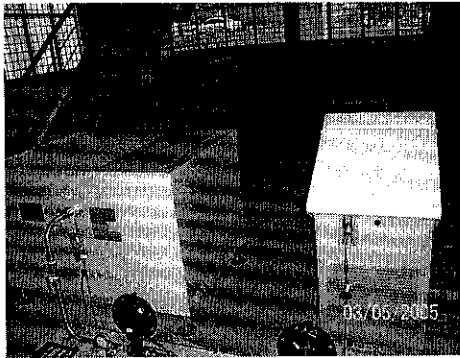


Figure 3-1e: Two compressors

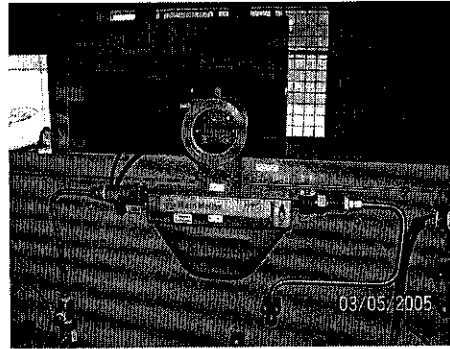


Figure 3-1f: Coriolis meter

Figure 3: Various parts of the NGV Dispenser Test Rig

3.1.2 Process Flow Description

In order to have better understanding on the process flow of the natural gas dispensing system, a Process & Instrumentation Diagram is included in this report (Refer to *Appendix 1-a*). However, to make it easier to observed the flow of the natural gas in the system, *Figure 4* is drew by eliminating some ball valves, check valves, relief valves, regulator valves, and some flow, pressure and temperature transmitters along the line. All of these valves and transmitters are not included in the diagram as they are not essential elements of the dispenser test rig.

Figure 4 portrays the simplified diagram of the natural gas dispensing system. As can be observed from the figure, materials or equipments are represented by tag numbers. These tag numbers will be defined individually in the process explanation and can also be referred in *Appendix 1-b*.

storage tanks. However, it is important to understand that when the dispensing occurs, the B240 hose should not be connected to the vehicle tank as shown in the figure. The hose is only connected to B070 and B110 valves when recycling system is operated. It means that, for dispensing system, while the first end of the vehicle tank is connected to nozzle, the other end is not connected to any other equipment. The natural gas flow goes into the vehicle tank where it accumulates. In this tank, pressure, temperature and mass of natural gas are measured using transmitters (B390, B450, and B460) as shown in the diagram. These transmitters will then send input signal to the data acquisition system (YC02). Data acquisition system will stores and displays all the data captured when requested by users.

There are three types of storage tank systems which consist of low bank, medium bank and high bank, designated as B280, B290, and B300 respectively. All of these tanks have the same pressure of 3600 psig when they are fully occupied by natural gas.

The natural gas dispensed from the low, medium or high bank will flow through a coriolis meter (B310). As shown in the diagram, the coriolis measured the flow of natural gas and using flow transmitter (B350) sends the measured value to the data acquisition system (YC-02). The natural gas then passes through three flow meters which are vortex, differential pressure and turbine meters. Since the meters are installed in a parallel arrangement, the natural gas is allowed to only flow only through any one of these meters at a time. In most of the experiment that have been conducted, only valves at the turbine flow meter are open to allow the flow of the natural gas. This indicates that the volumetric readings of the natural gas are measured by turbine meter which send the readings to the data acquisition system through flow transmitter. Turbine flow meter has been chosen as the flow dispenser flow meter because it offers reasonable performance at low cost. The turbine flow meter is a velocity measurement device, which rely on a uniform flow profile. Volumetric flow rate is calculated from the rotational speed of the turbine blade and the known pipe diameter. After flowing through the turbine meter, the natural gas finally flows through the flexible hose (B230) and nozzle (B250) into the vehicle tank.

Recycling process will take place to empty the vehicle tank that is filled with natural gas from the dispensing process. To operate the recycling system, flexible hose (B240) is used to connect vehicle tank to the temporary storage tanks (B270). One end of the high pressure flexible hose is coupled to a ball valve (B070) located at the bottom neck of the vehicle tank while the other end is connected to the inlet of a check valve (B110). Both valves B070 and B060 are then turned to 'ON' position. Gas will then flow into the temporary storage tanks which are also known as the recycling tanks. The start switch is then turned on which will start the recycling process. The gas from the recycling tanks flows to the compressor, usually B480. The other compressor (B470) acts as backup when B480 is under maintenance. Compressor is used to compress the gas which in turn provides the pressure different between the recycling tanks and the storage tanks. This is to ensure the flow from the recycling tanks to the storage tanks occur smoothly throughout the recycling process.

3.2 COMPUTATION OF ERROR FOR EOS

In order to achieve the objective to find the best suitable EOS that can be applied for natural gas in the system, computation of error for all EOS had been done. Several equations of state which are ideal gas, Virial, Van der Waal, Peng-Robinson, Soave-Redlich-Kwong and Lee-Kesler Plocker are used for this purpose. The computation of error in percentage is calculated using Microsoft Excel spreadsheet. An example of the spreadsheet can be viewed in *Appendix 2*. Several steps involved in the computation are summarized in *Figure 5*.

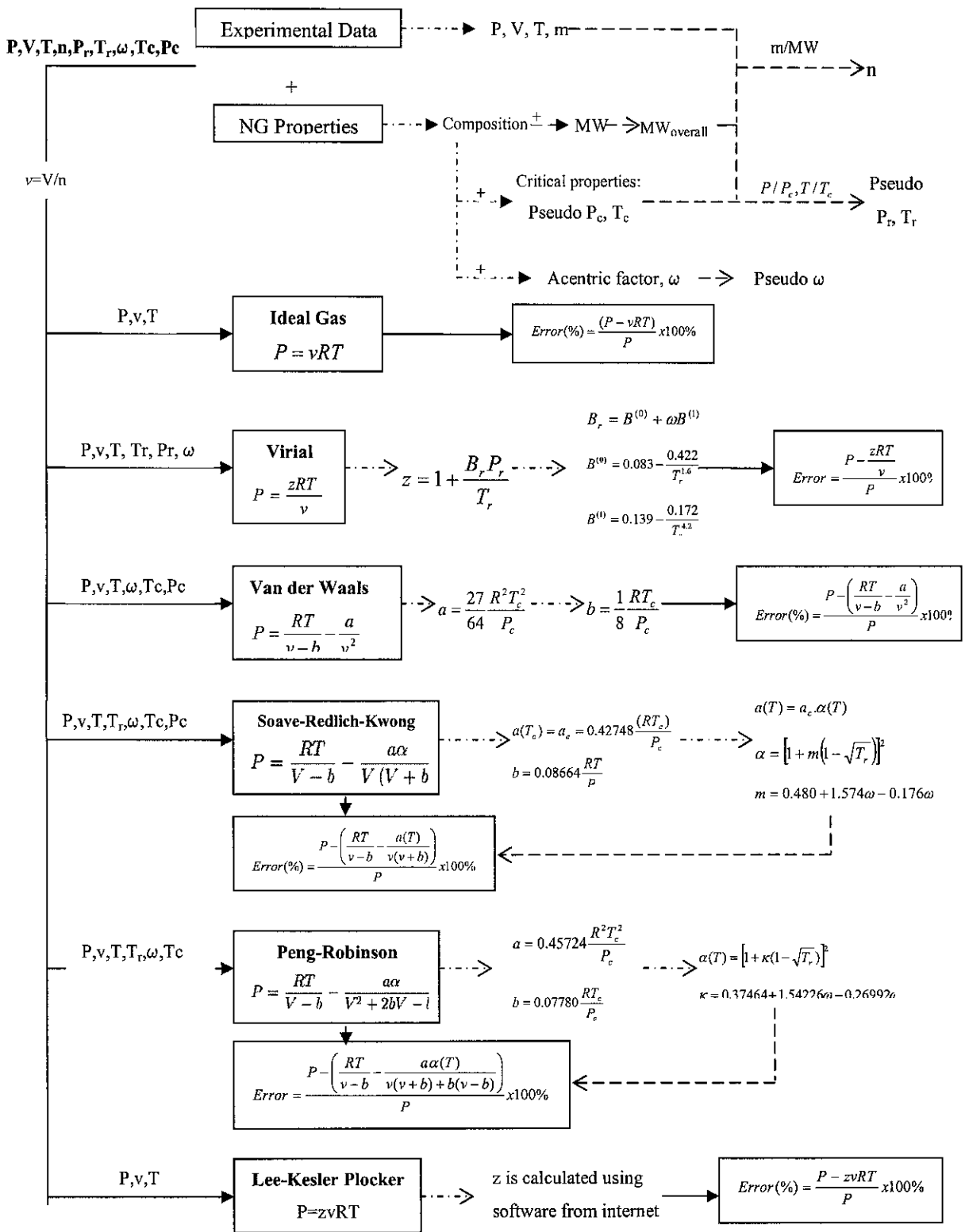


Figure 5: Steps for error computation of EOSs

In the early stage of the computation steps, experimental data along with Natural Gas properties were exploited to obtain some crucial data such as pressure (P), temperature (T) and volume (V) of the cylinder tank; number of mol (n); reduced pressure (P_r) and temperature (T_r); acentric factor (ω); and critical pressure (P_c) and temperature (T_c). Experiment conducted provides some important values that initiate the computation progress. The data that directly come from experiment conducted are pressure (P), temperature (T) and volume (V) of cylinder tank as well as mass of natural gas in the tank. In order to further develop the computation, some properties of natural gas need to be determined. Composition of the natural gas is the most critical data since other properties such as overall molecular weight (MW_{overall}); pseudo critical pressure (P_c) and temperature (T_c); and pseudo acentric factor (ω) can only be acquired from this data. Apart from the mentioned data, some data were exploited from experimental data and natural gas properties which resulted to number of mol (n) and pseudo reduced pressure (P_r) and temperature (T_r). After obtaining all these essential data, the computation proceeded with error computation for several EOS which involve Ideal Gas, Virial, Van der Waals, Soave-Redlich-Kwong, Peng-Robinson and Lee-Kesler Plocker equations. Having pictured the overall flow of the computation process, detailed equations or properties for some associated data are described in more detail in the next subsections.

3.2.1 Natural Gas Properties

Natural Gas Composition

Natural gas composition varies depending on the location where it is collected. For the purpose of this project, composition of natural gas is provided by Petronas Research and Scientific Service (PRSS). The composition was obtained from a study conducted by PRSS between Jun 1999 to January 2000 at various NGV dispensers as well as at Petronas Gas Berhad (PGB) Kapar. The natural gas studied was the one that had gone through treatment process where impurities such as sulfur, carbon dioxide and nitrogen were removed. The main component of the natural gas is thus methane. Other longer chain hydrocarbons such as ethane, propane, iso-butane and n-butane present in small amount. Although impurities had been extracted from the natural gas, some nitrogen and

carbon dioxide still exist in very small amount. *Table 2* shows the result of the study by categorizing the composition into the richest and the leanest.

Table 2: Compositions of Natural Gas (Leanest and Richest)

Gas Composition		Specification	
		Leanest (mol %)	Richest (mol %)
Methane	C1	96.42	89.04
Ethane	C2	2.29	5.85
Propane	C3	0.23	1.28
Iso-butane	iC4	0.03	0.14
n-butane	nC4	0.02	0.10
Iso-butane	iC5	n/a	n/a
n-pentane	nC5	n/a	n/a
n-hexane+	C6++	n/a	n/a
Condensate	C5+	0.00	0.02
Nitrogen	N2	0.44	0.47
Carbon dioxide	CO2	0.57	3.09
Gross Heating Value (GHV)		38.13	38.96

In order to use the composition data in the computation, average value between the leanest and the richest compositions need to be determined. The average value is computed using this equation:

$$Composition_{average} = \frac{Composition_{leanest} + Composition_{richest}}{2} \quad (3-1)$$

This result to average values for composition of natural gas as represented by *Table 3* which have been converted to mol fraction.

Table 3: Average Composition of Natural Gas

Component		Average Composition (mol fraction)
Methane	C1	0.92730
Ethane	C2	0.04070
Propane	C3	0.00755
Iso-butane	iC4	0.00085

n-butane	nC4	0.00060
Condensate	C5+	0.00010
Nitrogen	N2	0.00455
Carbon dioxide	CO2	0.01830

Molecular Weight of Natural Gas

Molecular weight is crucial to obtain the number of mol of the natural gas dispensed into the cylinder tank. Molecular weight of natural gas can only be determined by knowing its composition as well as molecular weight of its components. Molecular weight of every component in the natural gas is represented by **Table 4**.

Table 4: Molecular Weight of Natural Gas components

Component		Molecular Weight (kg/kmol)
Methane	C1	16.04
Ethane	C2	30.07
Propane	C3	44.10
Iso-butane	iC4	58.12
n-butane	nC4	58.12
Condensate	C5+	72.15
Nitrogen	N2	28.01
Carbon dioxide	CO2	44.01

Source: Perry's Chemical Engineers' Handbook

Using the average composition of natural gas that is calculated in the previous subsection, molecular weight of natural gas is computed using the following equation. From the calculation, the molecular weight of natural gas is then obtained

$$MW_{NG} = \sum (y_i)(MW_i) \quad (3-2)$$

where: y_i = molecular fraction of each component

MW_i = molecular weight of each component

Molecular weight and mass of the natural gas obtained from experimental data are exploited in order to determine the number of mol as shown by the equation below.

$$\text{Number of mol, } n = \frac{\text{mass, } m}{\text{molecular weight, } MW_{NG}} \quad (3-3)$$

Pseudo Critical Temperature and Pressure

As can be observed from **Figure 3-3**, critical properties such as critical pressure and critical temperature are very important in order to perform the computation. They are used for computation of error for Van der Waals, Soave-Redlich-Kwong and Peng-Robinson. Therefore, it is important to obtain the pseudo critical properties that can represent the natural gas. Pseudo critical properties of natural gas can only be computed by identifying the critical properties of its components as well as its composition. Critical properties of the various components in the natural gas are shown in **Table 5**.

Table 5: Critical Pressure and Temperature of Natural Gas Components

Component		Critical Pressure, Pc (kPa)	Critical Temperature, Tc (K)
Methane	C1	4600	190.6
Ethane	C2	4874	305.4
Propane	C3	4244	370.0
Iso-butane	iC4	3648	408.1
n-butane	nC4	3790	425.2
Condensate	C5+	3374	469.6
Nitrogen	N2	3384	126.2
Carbon dioxide	CO2	7376	304.2

Source: Chemical Engineering Thermodynamics

$$\text{Pseudocritical temperature, } T_{pc} = \sum (T_{ci})(y_i) \quad (3-4)$$

where T_{ci} = critical temperature of each component
 y_i = molecular fraction of each component

$$\text{Pseudocritical pressure, } P_{pc} = \sum (P_{ci})(y_i) \quad (3-5)$$

where P_{ci} = critical pressure of each component
 y_i = molecular fraction of each component

Method presented by Wichert and Aziz (1972) to correct the pseudo-critical properties of natural gases to the presence of non- hydrocarbon components, which is carbon dioxide is used. The correction factor is calculated using *Equation 2-10*. Since there is no H₂S presents in the natural gas, only coefficient A is inserted into the equation. Then, the corrected pseudo-critical properties P'_{pc} and T'_{pc} are calculated using *Equation 2-11 and 2-12*.

Acentric Factor, ω Computation

The value of acentric factor for each components of natural gas is represented by *Table 6*.

Table 6: Acentric factor of Natural Gas Components

Component		Acentric Factor, ω
Methane	C1	0.008
Ethane	C2	0.099
Propane	C3	0.152
Iso-butane	iC4	0.176
n-butane	nC4	0.193
Condensate	C5+	0.251
Nitrogen	N2	0.039
Carbon dioxide	CO2	0.225

Source: Chemical Engineering Thermodynamic

The pseudo acentric factor for natural gas is calculated as shown below:

$$\omega = \sum (\omega_i)(y_i) \quad (3-6)$$

where ω_i = acentric factor of each component

y_i = molecular fraction of each component

Conclusion of Natural Gas Properties

After performing all the calculations discussed earlier, properties of natural gas are obtained and summarized in *Table 7* below.

Table 7: Properties of Natural Gas

Property	Value
Molecular weight (kg/kgmol)	17.456
Critical Pressure (kPa)	4652
Critical Temperature (K)	199
Acentric factor	0.0172

3.2.4 Ideal Gas Error Computation

Computation of error for ideal gas equation is done by subtracting the right hand side term by left hand side term of equation. After that it is divided by one term of the equation and multiplied by 100 to obtain the percentage value as shown below:

$$Error = \frac{(P - vRT)}{P} \times 100\% \quad (3-7)$$

where

- P = pressure of tank (kPa)
- v = molar volume (m³/mol)
- T = temperature of tank (K)
- R = gas constant (8.314 m³.Pa/mol.K)

3.2.5 Van der Waals Error Computation

Error of Van der Waals is computed by using this equation:

$$Error(\%) = \frac{P - \left(\frac{RT}{v-b} - \frac{a}{v^2} \right)}{P} \times 100\% \quad (3-8)$$

where

$$a = \frac{27 R^2 T_c^2}{64 P_c}$$

$$b = \frac{1 R T_c}{8 P_c}$$

3.2.6 Peng-Robinson Error Computation

For Peng-Robinson, its error is represented by this equation:

$$\text{Error} = \frac{P - \left(\frac{RT}{v-b} - \frac{a\alpha(T)}{v(v+b) + b(v-b)} \right)}{P} \times 100\% \quad (3-9)$$

where $a = 0.45724 \frac{R^2 T_c^2}{P_c}$

$$b = 0.07780 \frac{RT_c}{P_c}$$

$$\alpha(T) = \left[1 + \kappa(1 - \sqrt{T_r}) \right]^2$$

$$\kappa = 0.37464 + 1.54226\omega - 0.26992\omega^2$$

The parameter ω is known as the acentric factor of the molecule and is a measure of its departure from perfectly spherical nature.

3.2.7 Soave-Redlich-Kwong (SRK) Error Computation

Equation to compute error of Soave-Redlich-Kwong equation is given below:

$$\text{Error (\%)} = \frac{P - \left(\frac{RT}{v-b} - \frac{a(T)}{v(v+b)} \right)}{P} \times 100\% \quad (3-10)$$

where $a(T_c) = a_c = 0.42748 \frac{(RT_c)^2}{P_c}$

$$b = 0.08664 \frac{RT}{P_c}$$

$$a(T) = a_c \cdot \alpha(T)$$

$$\alpha = \left[1 + m(1 - \sqrt{T_r}) \right]^2$$

$$m = 0.480 + 1.574\omega - 0.176\omega^2$$

3.2.8 Virial Error Computation

For Virial equation of state, error is computed using this equation:

$$Error = \frac{P - \frac{zRT}{P}}{P} \times 100 \% \quad (3-11)$$

where
$$z = 1 + \frac{B_r P_r}{T_r}$$

$$B_r = B^{(0)} + \omega B^{(1)}$$

$$B^{(0)} = 0.083 - \frac{0.422}{T_r^{1.6}}$$

$$B^{(1)} = 0.139 - \frac{0.172}{T_r^{4.2}}$$

$$P_r = \frac{P}{P_c}$$

$$T_r = \frac{T}{T_c}$$

3.2.9 Lee-Kesler Error Computation

Compressibility factor, z in this equation is computed using software downloaded from the internet, www.macatea.com. [14] as shown in **Figure 6** and **7**. In **Figure 6**, it is required to input certain values that are necessary for the computation. As can be observed from the figure, the values needed are critical temperature and pressure, acentric factor, and temperature and pressure of the fluid. **Figure 7** represents the results obtained after the computation by the software. The compressibility factor, z obtained is used for error computation using this equation:

$$Error(\%) = \frac{P - zvRT}{P} \times 100\% \quad (3-12)$$

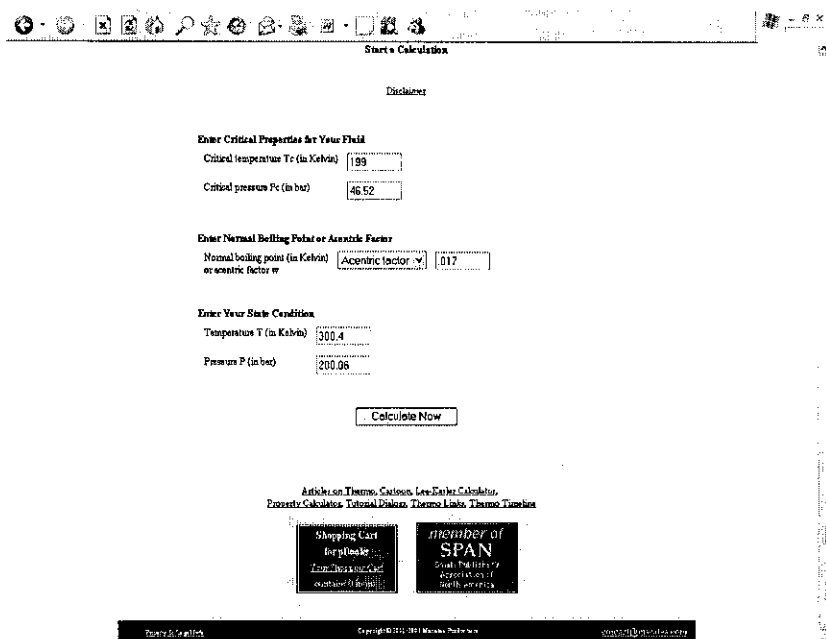


Figure 6: Data required by software

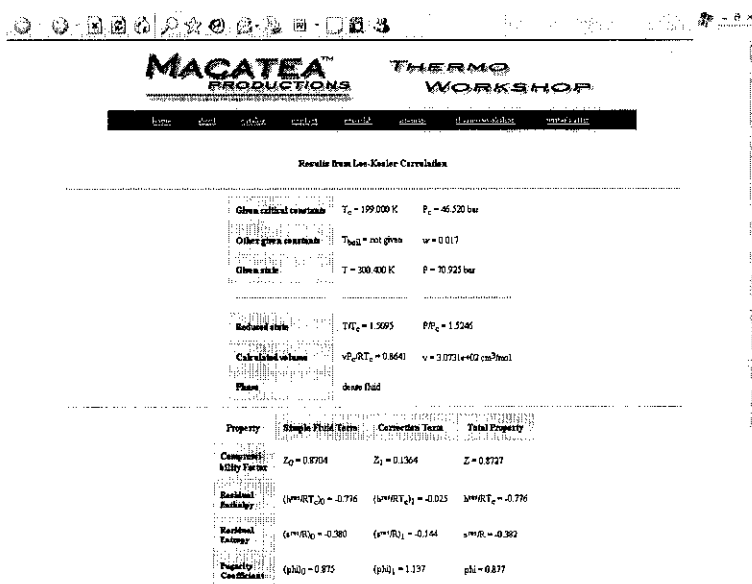


Figure 7: Results from computation

3.3 VALIDATION

After performing the computation of errors for all the tested EOSs, the EOS that gives the smallest error percentage is validated. In order to carry out the validation technique, mass flow rate is calculated based on the EOS and appropriate experimental data such as volumetric flow rate, pressure, temperature, and volume of tank. Having done this, the

mass flow rate calculated is then being compared to the one measured by coriolis meter. For the purpose of enhancing understanding on the steps taken, systematic flow of the steps are shown in *Figure 8*.

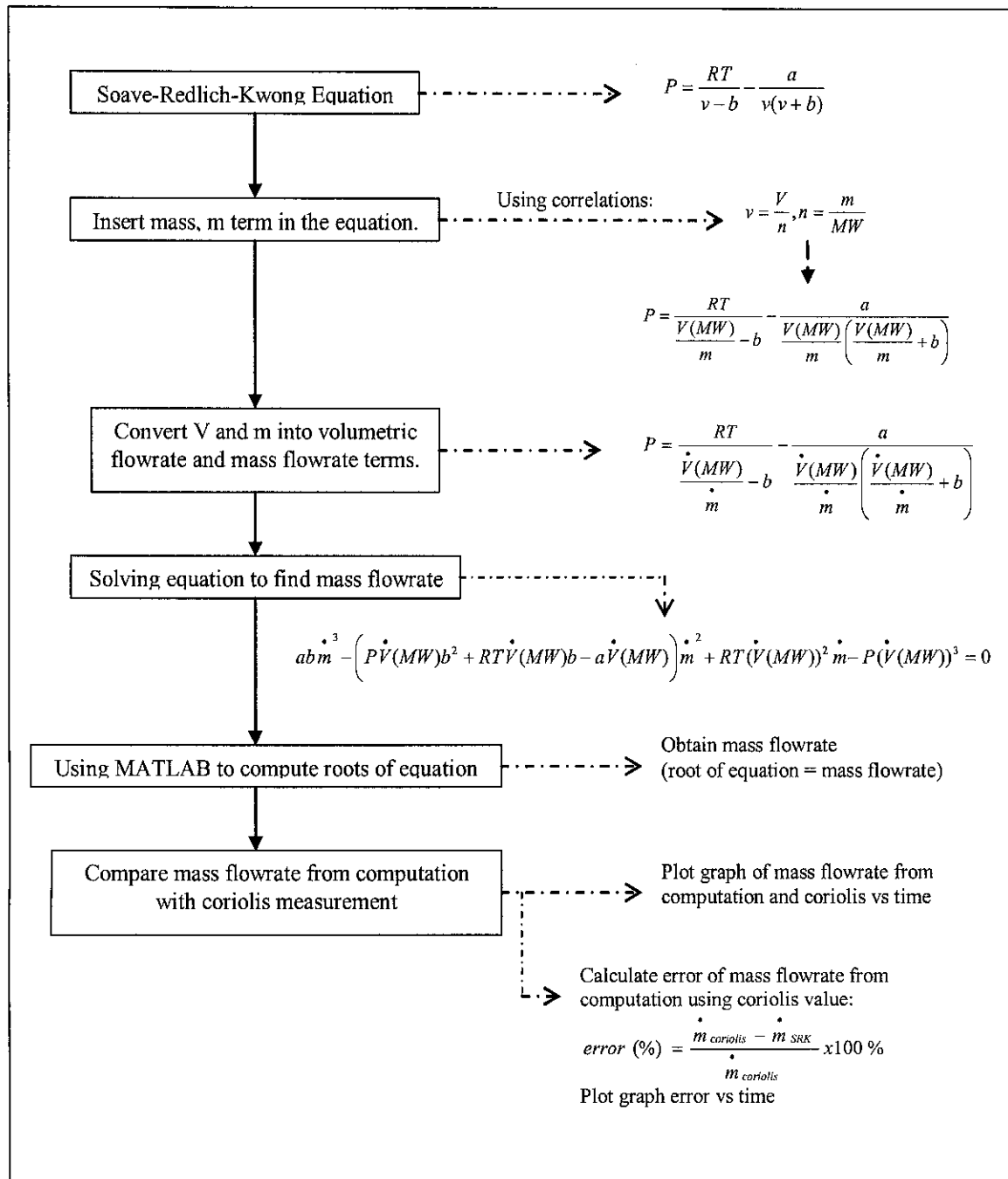


Figure 8: Systematic steps in validation technique

As can be observed in **Figure 8**, the first stage of validation technique is to identify the SRK equation of state. From this original equation, some manipulations are done to the input mass of natural gas term into the equation. Using the correlations shown below, equation with mass term is obtained:

$$v = \frac{V}{n} \quad (3-13)$$

$$n = \frac{m}{MW} \quad (3-14)$$

where v = volume per mol
 V = volume of tank
 n = number of mol of natural gas inside tank
 m = mass of natural gas inside tank
 MW = molecular weight of natural gas

After substituting the v and n terms with m term, the following equation is resulted:

$$P = \frac{RT}{\frac{V(MW)}{m} - b} - \frac{a}{\frac{V(MW)}{m} \left(\frac{V(MW)}{m} + b \right)} \quad (3-15)$$

Next the equation needs to be modified by inserting volumetric and mass flow rate terms into the equation. This is an important step since the objective is to find mass flow rate instead of mass of natural gas inside the tank to be compared with the one measured by coriolis meter. This step results to the following equation:

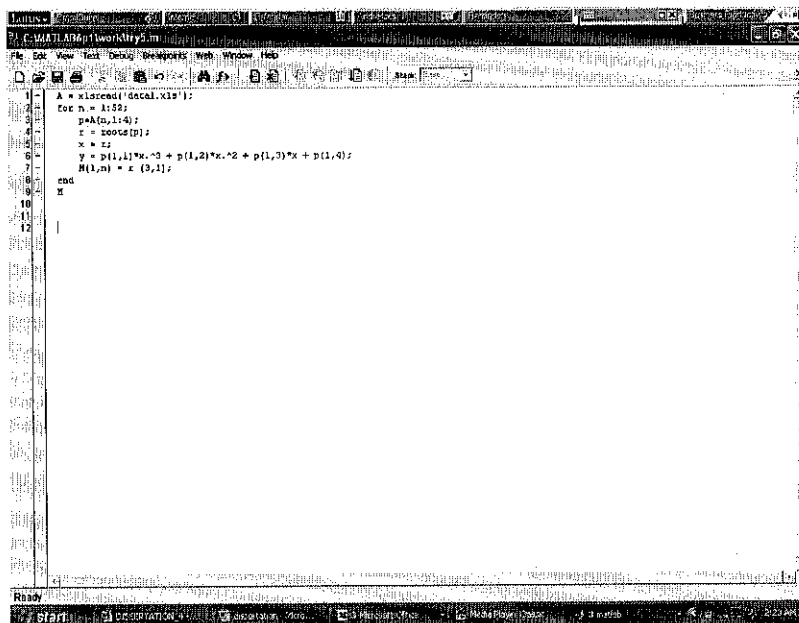
$$P = \frac{RT}{\frac{\dot{V}(MW)}{\dot{m}} - b} - \frac{a}{\frac{\dot{V}(MW)}{\dot{m}} \left(\frac{\dot{V}(MW)}{\dot{m}} + b \right)} \quad (3-16)$$

where \dot{V} = volumetric flow rate (m³/min)
 \dot{m} = mass flow rate (kg/min)

As shown in **Figure 8**, the validation technique continues by solving the SRK equation that has been modified by inserting mass flow rate and volumetric flow rate values. The calculation to solve this equation is shown in **Appendix 3**. From the calculation a polynomial equation as shown below is obtained.

$$ab \dot{m}^3 - \left(P \dot{V}(MW)b^2 + RT \dot{V}(MW)b - a \dot{V}(MW) \right) \dot{m}^2 + RT (\dot{V}(MW))^2 \dot{m} - P (\dot{V}(MW))^3 = 0 \quad (3-17)$$

The method to find the roots of this equation is quite challenging. However, with the aid of MATLAB program, this difficulty can be overcome. A command to find roots of polynomial equation is written in the MATLAB program as shown in **Figure 9** below. After this command is run, the result is obtained. An example of result obtained is represented by **Figure 10** which shows roots of equation for the first experiment. These roots of equation represent the mass flow rate of the natural gas.



```

1  A = x1stroot('dcal.x1st');
2  for n = 1:50;
3      pA(n,1:4);
4      r = roots(p);
5      x = r;
6      y = p(1,1)*x.^3 + p(1,2)*x.^2 + p(1,3)*x + p(1,4);
7      H(1,n) = x(3,1);
8  end
9
10
11
12

```

Figure 9: Command to find roots of equation using MATLAB program

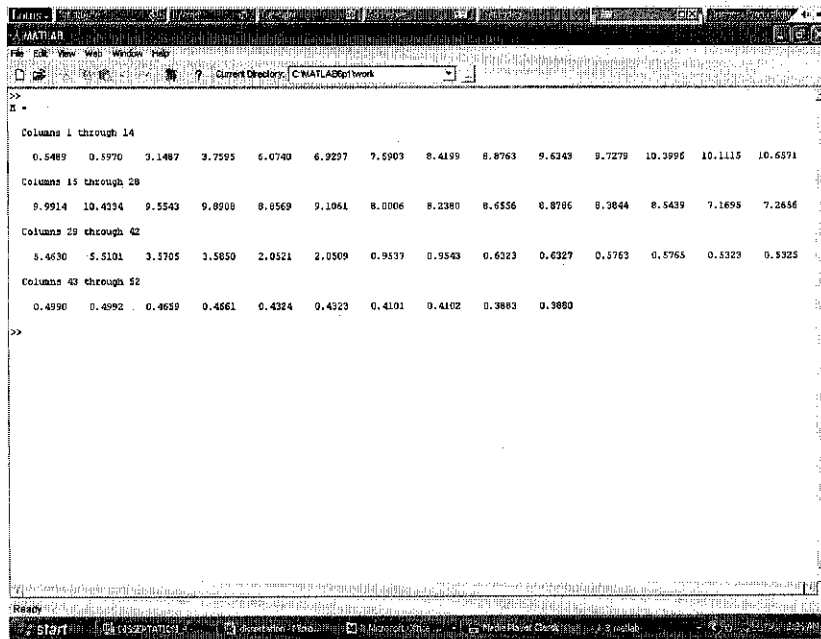


Figure 3. Roots of equation for the first experiment.

Finally, the mass flow rate obtained from the calculation is compared with the one measured by coriolis meter. Graph of both mass flow rates calculated from SRK equation and measured by coriolis versus time is plotted. The resulted curves are observed to identify how much value calculated from the EOS deviates from coriolis meter readings. Besides, error between those two values also being calculated. The equation is as follow:

$$error \ (%) = \frac{\dot{m}_{coriolis} - \dot{m}_{SRK}}{\dot{m}_{coriolis}} \times 100 \ \% \quad (3 - 18)$$

where

- $\dot{m}_{coriolis}$ = mass flow rate measured by coriolis meter
- \dot{m}_{SRK} = mass flow rate computed using SRK equation

CHAPTER 4

RESULTS AND DISCUSSION

Ten dynamic experiments and three static experiments had been conducted throughout this project. Data of these experiments were used in order to find the most suitable EOS that can represent the natural gas system. In the early stage of the project, dynamic experiments were conducted. However, the need for conducting static experiments arose when results obtained from the dynamic experiments did not meet the expectation.

4.1 DYNAMIC EXPERIMENT

Dynamic experiment in this project is defined as experiment that is conducted continuously, means natural gas is dispensed continuously into the vehicle tank. In this experiment, the Start Switch on the display panel is switched on and the natural gas is dispensed into the vehicle tank. The flow will stop automatically when there is no pressure difference between the storage tanks and the vehicle tank. However, there is another method of performing the dynamic experiment in this project. In the second method, the Start Switch is switched on to let the natural gas flow into the vehicle tank. After some time, the Start Switch is being turned off to stop the flow. Then, the natural gas inside the tank is allowed to stabilize inside the vehicle tanks for several seconds. The process is continued until the pressure inside the tank reaches its maximum value. Data of the dynamic experiments were collected using a data logging system, Read Win.

4.1.1 Experiment 1-4 (Single Continuous Flow of Natural Gas into the Vehicle Tank)

Data of pressure, temperature and mass of natural gas obtained from the experiments are used for calculation of errors of EOSs. The percentage errors are represented by *Figure 11-14*. From the figures, it is observed that the ideal gas equation gives the smallest errors

compared to others. It is followed by SRK, Lee-Kesler, Peng-Robinson, Van der Waals and Virial equations of state. All of the experiments (Experiment 1-4) give this same result. It is also observed that at one point in Experiment 2 (refer to *Figure 12*), a big deviation of percentage error occurred because the load cell (mass of the natural gas in the tank) increased excessively. There is a possibility that vibration in the surrounding causing a significant change in the mass detected by the load cell due to its sensitivity.

Overall, it can be observed that SRK, Lee-Kesler, PR, and Van der Waals give almost the same pattern. SRK, PR and Van der Waals are categorized into the cubic equation of state. These equations came from modification of ideal gas equation by including prediction of liquid phase formation. In general, they can provide reasonable values for both vapor and liquid regions of hydrocarbons and the vapor region for many other fluids. On the other hand, ideal gas and virial equations of state will never predict liquid phase formation, no matter what the temperature and pressure.

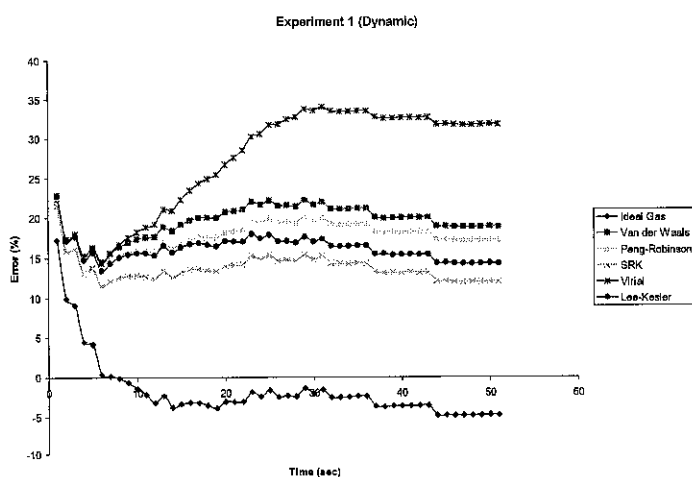


Figure11: Graph of error versus time for experiment 1

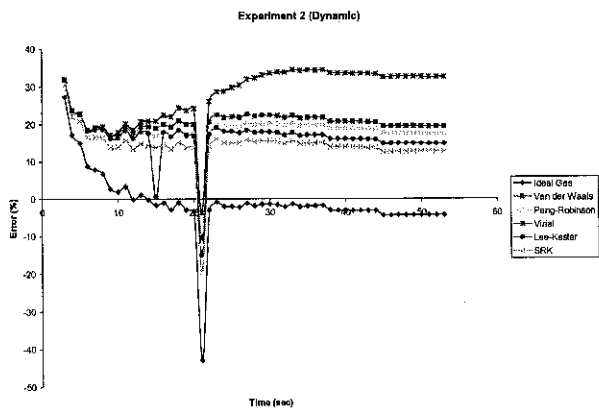


Figure 2: Graph of error versus time for experiment 2

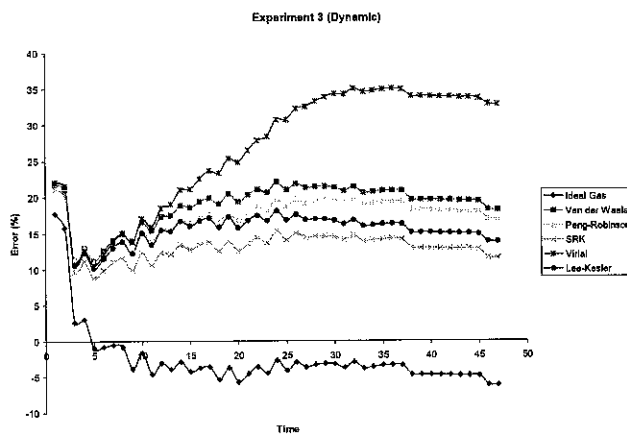


Figure 3: Graph of error versus time for experiment 3

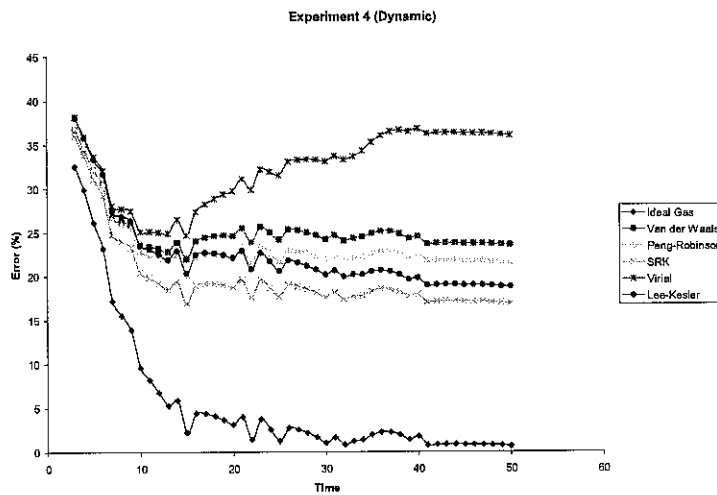


Figure 4: Graph of error versus time for experiment 4

At the very beginning of the experiments, the percentage errors for every equation give almost the same magnitude which is around 20-40 %. After this point, the percentage errors experienced a sudden decrease. The reason behind this behavior can be understood by observing the pressure, temperature and mass curves of the natural gas in the vehicle tank. Taking example of Experiment 1, the pressure, temperature and mass curves of the natural gas are shown in *Figure 15-17*. Pressure and mass of gas in the tank increases in a relatively constant manner as the tank receives an even amount of gas per unit of time. It is due to the fact that the amount of gas flowing into the tank is a function of the mass velocity of the gas flow. The temperature is constant at a magnitude of 303.3 K for the first 5 seconds. Before discussing the behavior of the temperature inside the tank, it should be noted that the temperature readings were taken digitally with one decimal point. Due to this fact, instead of a straight line, the curve as shown in *Figure 17* is obtained. Therefore, it can be assumed that there is a small gradual increment at the first 5 seconds. However, this increment could not be observed because it is less than 0.1K.

After about 25 seconds, the curves give systematic percentage errors especially for ideal gas, SRK, Lee-Kesler, PR, and Van der Waals equations. As can be observed from *Figure 15 and 16*, the pressure and mass of the natural gas inside the tank become constant after 25 seconds. At this period, the natural gas inside the tank had come to

reach its maximum capacity at pressure of 20 MPa. The flow became lesser which make the incremental of the mass become small.

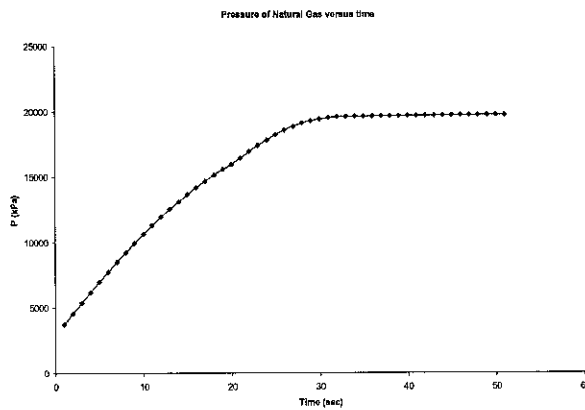


Figure 5: Graph of pressure inside the vehicle tank versus time for Experiment 1

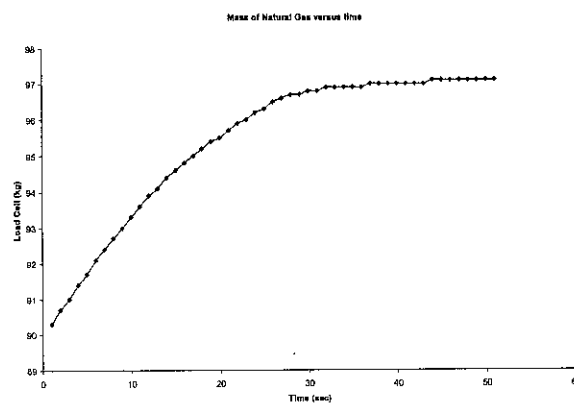


Figure 6: Graph of mass of natural gas versus time for Experiment 1

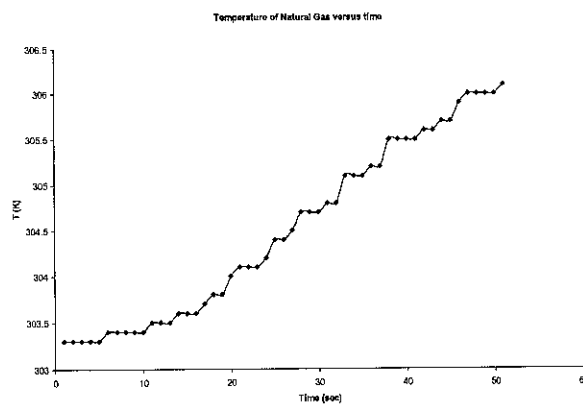


Figure 7: Graph of temperature inside the vehicle tank versus time for Experiment 1

4.1.2 Experiment 5 (Several Continuous Flow of Natural Gas into the Vehicle Tank)

For Experiment 5, natural gas is dispensed at the first 3 seconds of the experiment. After that the flow of the natural gas is stopped for about 45 seconds. Finally the natural gas is dispensed from 50-81 seconds until the maximum capacity of the tank is reached.

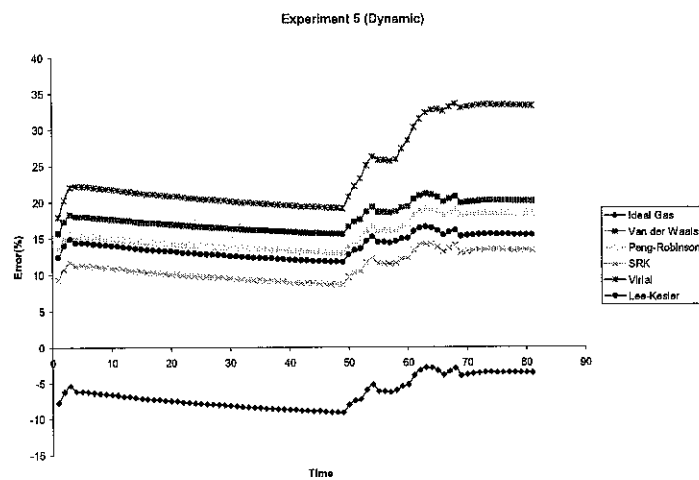


Figure 8: Graph of error versus time for experiment 5

The behaviors of pressure, mass and temperature of the natural gas inside the tank can be observed from *Figure 19-21*. In this experiment, we can clearly see that the percentage errors followed the same pattern with the pressure and mass of the natural gas. The result shows that the higher the pressure and mass of the natural gas inside the tank, the higher the percentage errors of the equations will be. This maybe due to the greater instability experienced by the natural gas as the pressure increases. As can be observed, the temperature keeps increasing inside the tank. This is due to collisions that occur inside the tank between molecules, as well as between molecules and the tank's wall.

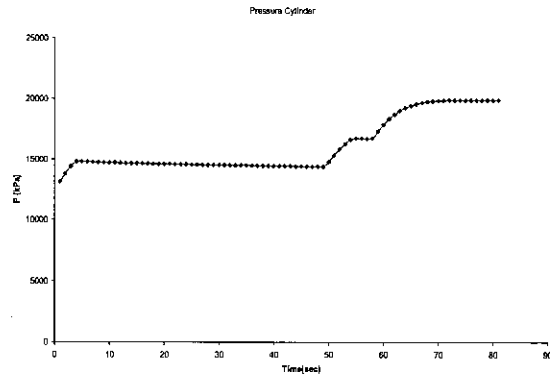


Figure 19: Graph of pressure inside the vehicle tank versus time for Experiment 5

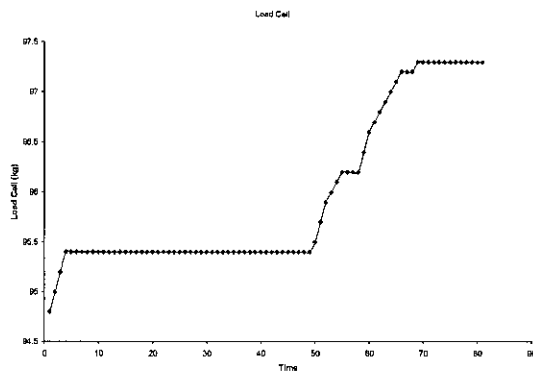


Figure 20: Graph of mass of natural gas versus time for Experiment 5

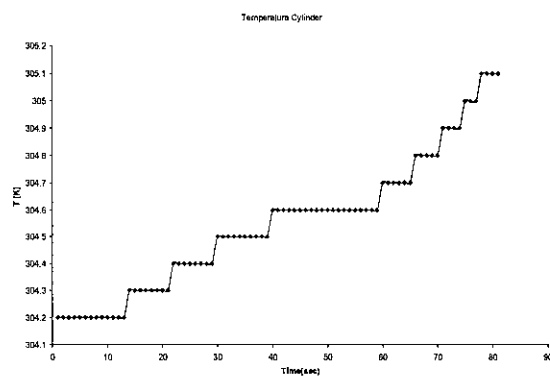


Figure 21: Graph of temperature inside the vehicle tank versus time for Experiment 5

Overall, the results obtained are unexpected because the ideal gas equation which is the very basic and general equation of state gives the smallest errors compare to others

extended equation of state. There are some factors that need to be considered in order to obtain more accurate result:

1. Vibration of load cell that effect the mass measurement of the NG inside the tank.
2. Mass of the natural gas inside the tank was recorded at only one decimal point which affects the accuracy of the calculation.

4.2 STATIC EXPERIMENT

In this project, static experiment is defined as experiment that is conducted without considering time as a factor. This means that natural gas is dispensed in small amount every time and all data such as pressure, temperature and mass of natural gas inside the tank is taken after a steady condition is reached.

Static experiments were run with the intention to compare the results obtain from the dynamic experiments. From the experiments conducted, results as shown in *Figure 22-24* were obtained. From the three experiments that had been conducted, SRK gives the smallest error followed by Lee-Kesler Plocker, Peng-Robinson, Van der Waals, Virial, and ideal gas equation. The results obtained from the static experiments are better compared to dynamic experiments because one of the factors that affect the accuracy of the results has been eliminated. The factor is the imprecise mass readings of the natural gas. In the static experiments, data were taken manually from the display panel which gives readings up to 3 decimal points. However, the accuracy of the temperature readings could not be improved since the temperature indicator in the display panel only gives readings at one decimal point.

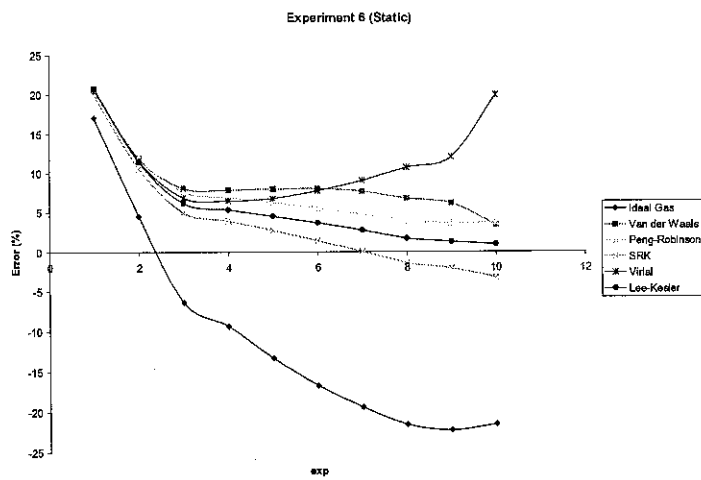


Figure 12: Graph of error versus time for experiment 6

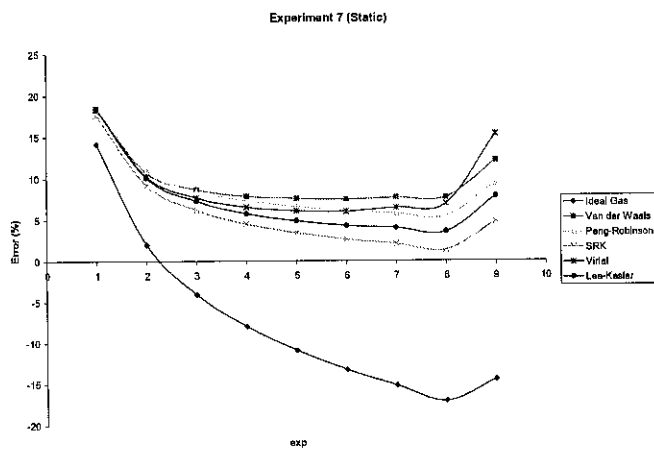


Figure 13: Graph of error versus time for experiment 7

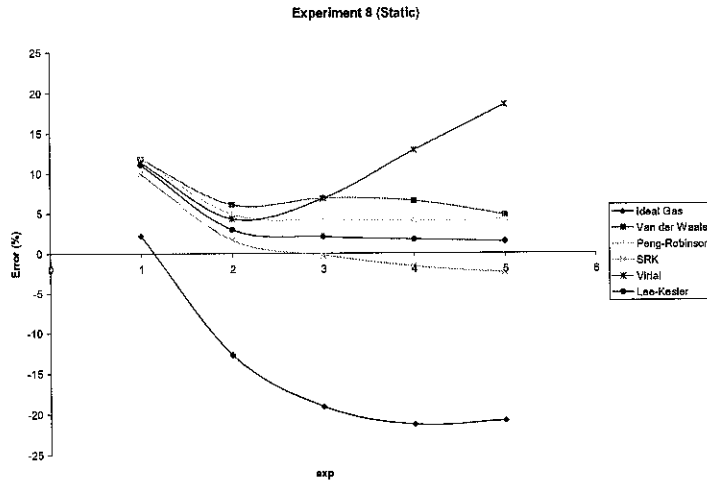


Figure 24: Graph of error versus time for experiment 8

The behavior of the pressure, mass and temperature of the natural gas inside the tank can be observed from *Figure 25-27*. The pressure, mass and temperature of the natural gas inside the tank increase gradually as the experiment was conducted. The natural gas was dispensed at approximately 2MPa in increment for every point until it reaches its maximum capacity, 20MPa as shown in *Figure 25*. The mass of the natural gas increases as the pressure increases due to the increments of the amount of the natural gas dispensed into the tank as shown in *Figure 26*. From *Figure 27*, it is observed that as the pressure increases, the temperature increases as well. This is due to the *Joule-Thompson Effect*. Joule-Thompson Effect indicates that at a moderate pressure, temperature decreases as pressure decreases and vice versa.

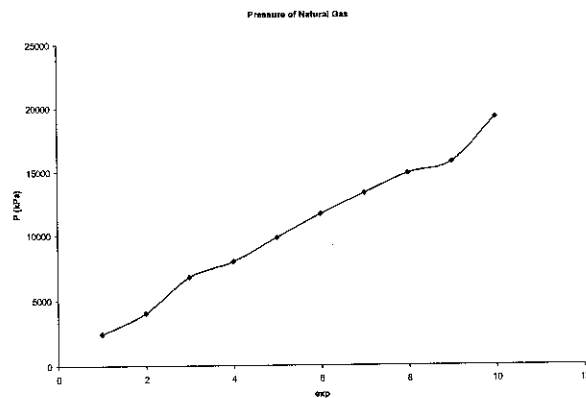


Figure 25: Pressure of NG inside the tank for Static Experiment (Exp. 6)

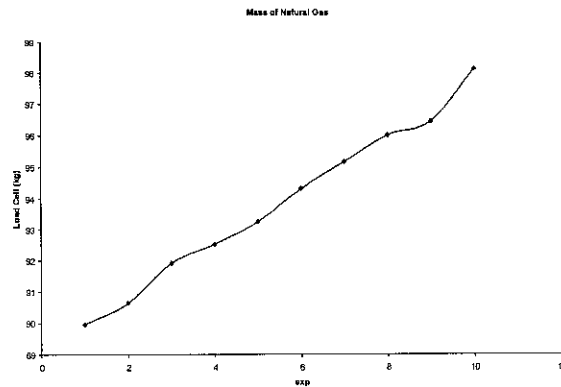


Figure 26: Mass of NG inside the tank for Static Experiment (Exp. 6)

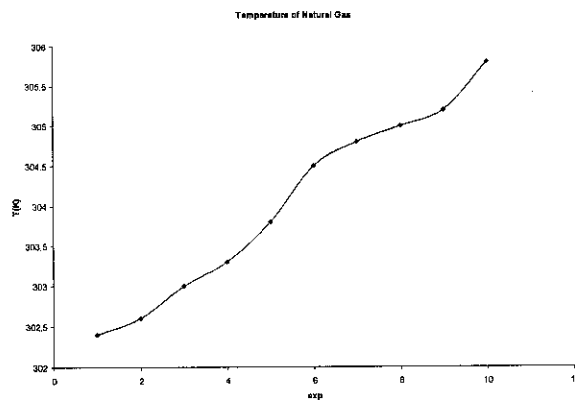


Figure 27: Temperature of NG inside the tank for Static Experiment (Exp. 6)

From experiments that had been conducted, SRK gives the smallest error in the static experiment and the second smallest error in the dynamic experiment. Therefore, it can be concluded that from all of the equations tested, SRK is the best equation to represent the natural gas. However, to prove the reliability of the SRK equation, a validation technique needs to be conducted.

4.3 VALIDATION

SRK is chosen as the best EOS for natural gas based on the results obtained from the experimental data and computation of errors. However, it is important to validate the result by comparing the mass flowrate calculated using SRK with the one measured by coriolis meter. To achieve this objective, volumetric flow rate readings from turbine

meter and mass flow rate readings from coriolis meter need to be collected. Only dynamics' experimental data can be used for the validation since in the static experiment, the volumetric and mass flow rate readings could not be obtained. After computation is done, the value of both mass flow rates is plotted as shown in *Figure 28*. Since all the dynamic experiments (Experiment 1-5) show the same observations, Experiment 1 is used for the purpose of explanation.

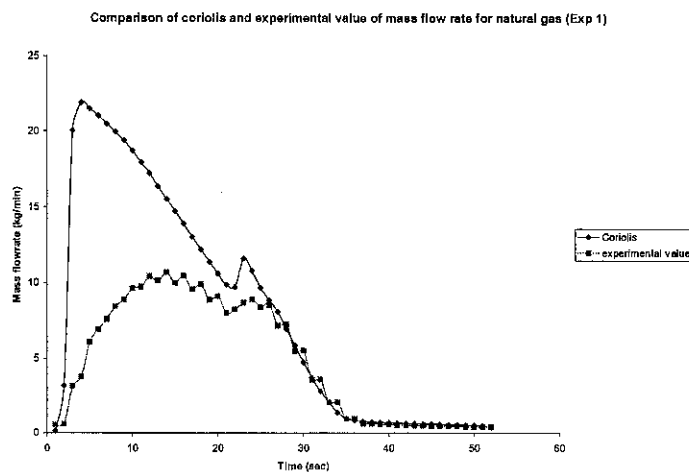


Figure 28: Comparison of coriolis and experimental value of mass flow rate for natural gas for Experiment 1

From the figure, both measurements give almost the same pattern. However, SRK gives poor indication of mass at the beginning of the experiment (1-25 seconds). Observing *Figure 15-17*, at the first 25 seconds of the experiment, pressure and mass of the natural gas increase gradually. The errors between the mass flow rates calculated using SRK from the actual mass flow rates measured by coriolis meter is possibly due to the unsteady condition experienced by the pressure inside the tank. This is because the natural gas was dispensed continuously. However towards the end of the experiment (26-51 seconds), the SRK gives good measurements of the mass flow rates. This is because the pressure inside the tank had reached its maximum value, 20MPa and began to reach its steady condition.

CHAPTER 5

CONCLUSIONS AND RECOMMENDATIONS

From the dynamic experiments conducted, the ideal gas law gives the smallest error percentage followed by SRK, Lee-Kesler, Peng-Robinson, Van der Waals and Virial equation of state. This result is improved by conducting static experiments, which conclude that SRK as the best EOS to represent natural gas followed by Lee-Kesler Plocker, Peng-Robinson, Van der Waals, Virial, and ideal gas equation. It is assumed that static experiments give more accurate results since all thermodynamic properties are taken at their steady state condition.

The result obtained is validated by comparing the mass flow rate obtained from calculation using SRK equation with measurements from coriolis meter. SRK gives good indication of mass flow rate toward the end of the experiment. At the very beginning of experiment, mass flow rate measured from SRK deviate from the actual mass flow rate as it gives low value of mass flow rate compared to the one measured by coriolis meter.

RECOMMENDATIONS FOR FUTURE WORK

For improvement, calculation using combination of several equation of state should be considered. The result might give a better data that can fit the real process much better compared to the single Equation of state. At some range of temperature and pressure, one EOS might be used and then at another range, the other EOS could be implemented.

Composition of natural gas in this project is obtained as average value from the leanest and the richest composition of natural gas that are provided by Petronas Research and Scientific Service (PRSS) from a study conducted by PRSS between Jun 1999 to January 2000. Because of this reason, composition of natural gas used may not exactly the same with the one prepared by the PRSS. It is best that a test to determine composition of natural gas is conducted specifically for the natural gas used in the experiment.

Since the results are affected by the poor parameter indicators in the experiment such as temperature and mass of the natural gas, it is best to use data acquisition system that can collect data as well as manipulated them to gives readings up to 3 decimal points. This should be done to achieve the accuracy of the calculations.

REFERENCES

R.L.Bechtold, (1997, March), *Alternative Fuels for Vehicle Fleet Demonstration Program (Volume 1)*.

Karl Stappert, *Mass Meters for Gas Measurement*.

J.F.Estela-Urbe, J.Jaramillo, M.A. Salazar, J.P.M. Trusler (2002), *Virial Equation of State for Natural Gas Systems*.

Jack Winnick, (1997), *Chemical Engineering Thermodynamics*; John Wiley & Sons, Inc.

Sandler, I. Stanley (1999), *Chemical and Engineering Thermodynamics (Third Edition)*; John Wiley & Sons, Inc.

Calculation software for Lee-Kesler-Plocker Equation of State.

<<http://www.macatea.com/workshop/>>.

W.F. Stewart, S.F. Burkhardt, D. Voo, in: Proceedings of the Presentation the AIChE Meeting, Kansas City, MO, 1959.

R.P. Sutton, in: Proceedings of the Presentation of the Annual Technology Conference Exhibition, Las Vegas, NV, 22–25 September 1985, paper SPE 14265.

E. Wichert, K. Aziz, *Hydrocarbon Proces.* 51 (5) (1972) 119–122.

M.B. Standing, D.L. Katz, *Trans. AIME* 146 (1942) 140–149.

APPENDICES

APPENDIX 1-b

Table 1-b : Bill of Material of NGV test rig

ITEM	DESCRIPTION	QTY.	MATERIAL/SPECIFICATION
B010	VALVE, BALL	3	PARKER P/N: HPB688A
B020	VALVE, BALL	8	PARKER P/N: HPB688FF
B030	VALVE, BALL	2	KITZ BRASS 150PSIG MAMP
B040	VALVE, BALL	1	SWAGelok P/N: SS-63T58
B050	VALVE, BALL	3	SWAGelok P/N: SS-33VF4
B060	VALVE, BALL	1	SWAGelok P/N: SS-83K58
B070	VALVE, BALL	1	QASIS P/N: BV506-NI
B075	VALVE, BALL	4	PARKER P/N: 4A-B2LJ2-SSP
B080	VALVE, BALL PNEUMATIC	3	PARKER P/N: 8A-BBLJ2-SSP-62AC-3
B090	VALVE, BALL PNEUMATIC	2	PARKER P/N: 8F-BBLJ2-SSP-62AC-3
B100	VALVE, CHECK	3	PARKER P/N: 8A-CBL-1-SS
B110	VALVE, CHECK	3	SWAGelok P/N: SS-CHS16-1
B120	VALVE, CHECK	2	SWAGelok P/N: SS-CHS4-1
B130	VALVE, CHECK	4	PARKER P/N: 4A-C4L-1-SS
B140	VALVE, NEEDLE	1	AGCO P/N: H5RIC-22
B150	VALVE, NEEDLE	1	SWAGelok P/N: SS-1FS4
B160	VALVE, NEEDLE	3	PARKER P/N: 4A-V4LN-SS
B170	VALVE, RELIEF	1	SWAGelok P/N: SS-4R3A1 SET @ 3750PSIG
B180	VALVE, RELIEF	3	SWAGelok P/N: SS-4R3A SET @ 3950PSIG
B185	VALVE, RELIEF	1	SWAGelok P/N: SS-RL4MBFB SET @ 100PSIG
B190	VALVE, REGULATOR	1	JORDAN P/N: JHR Cv=0.6 SET @ 150PSIG
B200	VALVE, REGULATOR	1	JORDAN P/N: JHR Cv=0.6 SET @ 30PSIG
B210	VALVE, REGULATOR	1	JORDAN P/N: MARK608 5/16" OR SET @ 7" H2O
B220	VALVE, REGULATOR	1	JORDAN P/N: MARK808 3/16" OR SET @ 35" H2O
B230	HOSE, FLEXIBLE	1	SWAGelok P/N: SS-NGS6-NN-120X
B240	HOSE, FLEXIBLE	1	PARKER P/N: 80NG0101-16-16-16-120
B250	NOZZLE	1	SWAGelok P/N: SS-83KKF4
B260	CYLINDER, NGV	1	EKC 1X55LWC 3600PSIG
B270	CYLINDER, NGV	1	EKC 3X55LWC 3600PSIG
B280	CYLINDER, NGV	1	EKC 4X55LWC 3600PSIG LOW BANK
B280	CYLINDER, NGV	1	EKC 3X55LWC 3600PSIG MEDIUM BANK
B300	CYLINDER, NGV	1	EKC 2X55LWC 3600PSIG HIGH BANK
B310	FLOW, SENSOR CORIOLIS	1	MICROMOTION P/N: CMG050239K-AZEZZZ
B320	FLOW, SENSOR TURBINE	1	HOFFER P/N: 3/4X3/4-25-CB-1RPR-MS-CE
B330	FLOW, SENSOR ORIFICE	1	ENDRESS + HAUSER P/N: DN25 PN250
B340	FLOW, SENSOR VORTEX	1	ENDRESS + HAUSER P/N: 70HS25-DDD20B1B100
B350	FLOW, TRANSMITTER CORIOLIS	1	MICROMOTION P/N: 2700011BBFEZZZ
B360	FLOW, TRANSMITTER TURBINE	1	HOFFER P/N: HIT2A-3-B-C-X-FX
B370	FLOW, TRANSMITTER ORIFICE	1	ENDRESS + HAUSER P/N: PM0235-MBS86EM3C
B380	FLOW, TRANSMITTER VORTEX	1	ENDRESS + HAUSER P/N: 70HS25-DDD20B1B100
B390	PRESSURE, TRANSMITTER	3	ENDRESS + HAUSER P/N: PMP731-133Z1M21X1

ITEM	DESCRIPTION	QTY.	MATERIAL/SPECIFICATION
B400	PRESSURE, TRANSMITTER	2	MURPHY P/N: PXMS-6000
B410	PRESSURE, TRANSMITTER	5	MURPHY P/N: PXMS-5000
B420	PRESSURE, GAUGE	1	SWAGELOK P/N:
B430	PRESSURE, GAUGE	4	SWAGELOK P/N:
B440	PRESSURE, GAUGE	2	ASHCROFT 2-1/2" DIAL 0-60" H2O
B450	TEMPERATURE, TRANSMITTER	3	ENDRESS + HAUSER P/N: TMT162-E21231AAA
B460	LOAD CELL	1	METTLER TOLEDO EX APPROVED, 0-150KG
B470	COMPRESSOR, TIME FILLED	1	FUEL MAKER P/N: FMQ-2-36
B480	COMPRESSOR, TIME FILLED	1	FUEL MAKER P/N: FMQ-B-36
YC-01	DISPENSER REGISTER	1	KRAUS P/N: 09 NZBAGUCGMS-D
YC-02	DATA ACQUISITION SYSTEM	1	ENDRESS + HAUSER P/N: RSG10-B162CZ188

APPENDIX 2

Data

Volume of tank=	0.0563	m ³
Initial weight of tank=	89.1	kg
Gas constant=	8.314	m ³ kPa/kmol K

Properties of NG

Component	Composition		MW	Tc(K)	Pc(kPa)	ω
	Leanest	Richest				
C1	0.9642	0.8905	16.04	190.6	4600	0.008
C2	0.0229	0.0585	30.07	305.4	4874	0.099
C3	0.0023	0.0128	44.10	370	4244	0.152
iC4	0.0003	0.0014	58.12	408.1	3648	0.176
nC4	0.0002	0.001	58.12	425.2	3790	0.193
C5+	0	0.0002	72.15	469.6	3374	0.251
N2	0.0044	0.0047	28.01	126.2	3384	0.039
CO2	0.0057	0.0309	44.01	304.2	7376	0.225

Total MW: Leanest= 16.66 Average= 17.4558 kg/kmol
 Richest= 18.25

Tc for Natural Gas: Leanest= 194 Average= 199 K
 Richest= 203

Pc for Natural Gas: Leanest= 4615 Average= 4652 kPa
 Richest= 4689

Acentric factor, ω : Leanest= 0.012 Average= 0.017
 Richest= 0.022

Van der Waals Coefficients: a= 247.640
 b= 0.044

Peng-Robinson Coefficients: a= 268.399
 b= 0.028
 K= 0.401

Soave-Redlich-Kwong Coefficients: b= 0.031
 m= 0.507

Date/Time	Load Cell Kg	Pres Cyl kPa	Temp Cyl K	v		Ideal Gas Error(%)	Van der Waals Error(%)		Peng-Robinson $\alpha(T)$ Error(%)		Soave-Redlich-Kwong $\alpha(T)$ Error(%)		Virial z Error(%)		Lee-Kesler z Error(%)	
				Pr	Tr								Br	z		z
1/31/2005 16:26	90.3	3438	303.3	0.739	1.526	0.819	16	16	0.820	16	0.776	194.6	-0.130	0.937	16	0.9382
1/31/2005 16:26	90.3	3721	303.3	0.800	1.526	0.819	22	22	0.820	23	0.776	194.6	-0.130	0.932	23	0.9333
1/31/2005 16:26	90.7	4555	303.3	0.979	1.526	0.614	17	17	0.820	17	0.776	194.6	-0.130	0.917	17	0.9189
1/31/2005 16:26	91	5362	303.3	1.153	1.526	0.517	18	18	0.820	18	0.776	194.6	-0.130	0.902	18	0.9054
1/31/2005 16:26	91.4	6176	303.3	1.327	1.526	0.427	15	15	0.820	15	0.776	194.6	-0.130	0.887	15	0.8921
1/31/2005 16:26	91.7	6962	303.3	1.496	1.526	0.378	16	16	0.820	16	0.776	194.6	-0.130	0.873	16	0.8798
1/31/2005 16:26	92.1	7727	303.4	1.661	1.526	0.328	15	15	0.820	14	0.775	194.6	-0.130	0.859	14	0.8686
1/31/2005 16:26	92.4	8485	303.4	1.824	1.526	0.298	16	16	0.820	15	0.775	194.6	-0.130	0.832	17	0.8579
1/31/2005 16:26	92.7	9230	303.4	1.984	1.526	0.273	17	17	0.820	16	0.775	194.6	-0.130	0.819	18	0.8481
1/31/2005 16:26	93	9940	303.4	2.137	1.526	0.252	18	18	0.820	16	0.775	194.6	-0.130	0.806	18	0.8395
1/31/2005 16:26	93.3	10630	303.4	2.285	1.526	0.234	17	17	0.820	16	0.775	194.6	-0.130	0.794	19	0.8319
1/31/2005 16:26	93.6	11305	303.5	2.430	1.527	0.218	18	18	0.820	16	0.775	194.5	-0.130	0.782	19	0.8254
1/31/2005 16:26	93.9	11940	303.5	2.586	1.527	0.205	18	18	0.820	16	0.775	194.5	-0.130	0.771	21	0.8199
1/31/2005 16:26	94.1	12546	303.5	2.697	1.527	0.197	19	19	0.820	17	0.775	194.5	-0.130	0.761	21	0.8153
1/31/2005 16:26	94.4	13112	303.6	2.818	1.527	0.185	18	18	0.820	16	0.775	194.5	-0.129	0.751	21	0.8119
1/31/2005 16:26	94.6	13663	303.6	2.937	1.527	0.179	19	19	0.820	17	0.775	194.5	-0.129	0.742	22	0.8089
1/31/2005 16:26	94.8	14187	303.6	3.049	1.527	0.172	20	20	0.820	17	0.775	194.5	-0.129	0.733	23	0.8066
1/31/2005 16:26	95	14684	303.7	3.156	1.528	0.167	20	20	0.820	18	0.775	194.5	-0.129	0.725	24	0.8052
1/31/2005 16:26	95.2	15139	303.8	3.254	1.528	0.161	20	20	0.819	18	0.775	194.4	-0.129	0.717	25	0.8044
1/31/2005 16:26	95.4	15580	303.8	3.349	1.528	0.156	20	20	0.819	18	0.775	194.4	-0.129	0.711	25	0.8036
1/31/2005 16:26	95.5	15966	304	3.432	1.529	0.154	21	21	0.819	18	0.774	194.3	-0.129	0.702	27	0.8038
1/31/2005 16:26	95.7	16462	304.1	3.539	1.530	0.149	21	21	0.819	18	0.774	194.3	-0.129	0.702	28	0.8039
1/31/2005 16:26	95.9	16966	304.1	3.647	1.530	0.145	21	21	0.819	19	0.774	194.3	-0.129	0.693	29	0.8042
1/31/2005 16:26	96	17428	304.1	3.746	1.530	0.142	22	22	0.819	20	0.774	194.3	-0.129	0.685	30	0.8048
1/31/2005 16:26	96.2	17841	304.2	3.835	1.530	0.138	22	22	0.819	19	0.774	194.2	-0.129	0.677	31	0.8059
1/31/2005 16:26	96.3	18234	304.4	3.919	1.531	0.136	22	22	0.819	20	0.774	194.1	-0.128	0.671	32	0.8075
1/31/2005 16:26	96.5	18593	304.4	3.996	1.531	0.133	22	22	0.819	19	0.774	194.1	-0.128	0.665	32	0.8086
1/31/2005 16:26	96.6	18882	304.5	4.059	1.532	0.131	22	22	0.818	20	0.773	194.1	-0.128	0.660	32	0.8099
1/31/2005 16:26	96.7	19131	304.7	4.112	1.533	0.129	21	21	0.818	19	0.773	194.0	-0.128	0.656	33	0.8114

1/31/2005 16:27	96.7	19317	304.7	4.152	1.533	0.129	-1	22	0.818	20	0.773	194.0	15	-0.128	0.653	34	0.8122	18
1/31/2005 16:27	96.8	19448	304.7	4.180	1.533	0.128	-2	22	0.818	20	0.773	194.0	15	-0.128	0.651	34	0.8127	17
1/31/2005 16:27	96.8	19551	304.8	4.202	1.533	0.128	-2	22	0.818	20	0.773	194.0	15	-0.128	0.649	34	0.8135	17
1/31/2005 16:27	96.9	19606	304.8	4.214	1.533	0.126	-3	21	0.818	19	0.773	194.0	14	-0.128	0.648	34	0.8137	17
1/31/2005 16:27	96.9	19634	305.1	4.220	1.535	0.126	-3	21	0.818	19	0.772	193.8	14	-0.128	0.649	33	0.8146	16
1/31/2005 16:27	96.9	19641	305.1	4.222	1.535	0.126	-3	21	0.818	19	0.772	193.8	14	-0.128	0.649	33	0.8146	17
1/31/2005 16:27	96.9	19655	305.1	4.225	1.535	0.126	-2	21	0.818	19	0.772	193.8	14	-0.128	0.649	34	0.8147	17
1/31/2005 16:27	96.9	19662	305.2	4.226	1.535	0.126	-2	21	0.817	19	0.772	193.8	14	-0.128	0.649	34	0.8150	17
1/31/2005 16:27	97	19675	305.2	4.229	1.535	0.124	-4	20	0.817	18	0.772	193.8	13	-0.128	0.649	33	0.8150	16
1/31/2005 16:27	97	19682	305.5	4.231	1.537	0.124	-4	20	0.817	18	0.772	193.6	13	-0.127	0.650	33	0.8142	16
1/31/2005 16:27	97	19689	305.5	4.232	1.537	0.124	-4	20	0.817	18	0.772	193.6	13	-0.127	0.650	33	0.8158	15
1/31/2005 16:27	97	19696	305.5	4.234	1.537	0.124	-4	20	0.817	18	0.772	193.6	13	-0.127	0.649	33	0.8159	15
1/31/2005 16:27	97	19703	305.5	4.235	1.537	0.124	-4	20	0.817	18	0.772	193.6	13	-0.127	0.649	33	0.8159	15
1/31/2005 16:27	97	19710	305.6	4.237	1.537	0.124	-4	20	0.817	18	0.771	193.6	13	-0.127	0.650	33	0.8162	15
1/31/2005 16:27	97	19717	305.6	4.238	1.537	0.124	-4	20	0.817	18	0.771	193.6	13	-0.127	0.650	33	0.8162	15
1/31/2005 16:27	97.1	19731	305.7	4.241	1.538	0.123	-5	19	0.817	17	0.771	193.5	12	-0.127	0.650	32	0.8166	14
1/31/2005 16:27	97.1	19737	305.7	4.242	1.538	0.123	-5	19	0.817	17	0.771	193.5	12	-0.127	0.650	32	0.8166	14
1/31/2005 16:27	97.1	19744	305.9	4.244	1.539	0.123	-5	19	0.816	17	0.771	193.5	12	-0.127	0.650	32	0.8171	14
1/31/2005 16:27	97.1	19751	306	4.245	1.539	0.123	-5	19	0.816	17	0.771	193.4	12	-0.127	0.651	32	0.8174	14
1/31/2005 16:27	97.1	19751	306	4.245	1.539	0.123	-5	19	0.816	17	0.771	193.4	12	-0.127	0.651	32	0.8174	14
1/31/2005 16:27	97.1	19758	306	4.247	1.539	0.123	-5	19	0.816	17	0.771	193.4	12	-0.127	0.651	32	0.8174	14
1/31/2005 16:27	97.1	19772	306	4.250	1.539	0.123	-5	19	0.816	17	0.771	193.4	12	-0.127	0.650	32	0.8175	14
1/31/2005 16:27	97.1	19772	306.1	4.250	1.540	0.123	-5	19	0.816	17	0.771	193.4	12	-0.127	0.651	32	0.8178	14

APPENDIX 3

CALCULATION STEPS FOR SRK EQUATION TO SOLVE FOR MASS FLOWRATE

$$\begin{aligned}
 P &= \frac{RT}{\frac{\dot{V}(MW)}{m} - b} - \frac{a}{\frac{\dot{V}(MW)}{m} \left(\frac{\dot{V}(MW)}{m} + b \right)} \\
 P \left(\frac{\dot{V}(MW)}{m} - b \right) &= RT - \frac{a \left(\frac{\dot{V}(MW)}{m} - b \right)}{\frac{\dot{V}(MW)}{m} \left(\frac{\dot{V}(MW)}{m} + b \right)} \\
 P \left(\frac{\dot{V}(MW)}{m} - b \right) \frac{\dot{V}(MW)}{m} \left(\frac{\dot{V}(MW)}{m} + b \right) &= RT \frac{\dot{V}(MW)}{m} \left(\frac{\dot{V}(MW)}{m} + b \right) - a \left(\frac{\dot{V}(MW)}{m} - b \right) \\
 P \left(\frac{\dot{V}(MW)}{m} \right)^3 - Pb^2 \frac{\dot{V}(MW)}{m} + Pb \left(\frac{\dot{V}(MW)}{m} \right)^2 - P \left(\frac{\dot{V}(MW)}{m} \right) &= RT \left(\frac{\dot{V}(MW)}{m} \right)^2 - a \frac{\dot{V}(MW)}{m} + ab \\
 P \left(\frac{\dot{V}(MW)}{m} \right)^3 - Pb^2 \frac{\dot{V}(MW)}{m} + Pb \left(\frac{\dot{V}(MW)}{m} \right)^2 - P \left(\frac{\dot{V}(MW)}{m} \right) &= RT \left(\frac{\dot{V}(MW)}{m} \right)^2 - a \frac{\dot{V}(MW)}{m} + ab \\
 abm - \left(P \frac{\dot{V}(MW)}{m} \right)^3 + RT \frac{\dot{V}(MW)}{m} b - a \frac{\dot{V}(MW)}{m} &= 0
 \end{aligned}$$